TGAL-TR-83-5

EVALUATION OF THE RSTN NETWORK AND FURTHER IMPROVEMENT TO AUTOMATIC ASSOCIATION

R.R. Blandford, J. Goncz, R. Baumstark, and K.L. McLaughlin

TELEDYNE GEOTECH
Alexandria Laboratories
314 Montgomery Street
Alexandria, VA 22314

30 October 1983

Technical Report

DTIC
ELECTE
OCT 0 4 1984
E

84 10 03 078

REPORT DOCUMENTATION PAGE

1. REPORT SECURITY CLASSIFICATION		1b. RESTRICTIVE MARKINGS
Unclassified		
2a. SECURITY CLASSIFICATION AUTHORITY		3. DISTRIBUTION/AVAILABILITY OF REPORT
		APPROVED FOR PUBLIC RELEASE;
2b. DECLASSIFICATION/DOWNGRADING SCHEDULE		DISTRIBUTION UNLIMITED.

4. PERFORMING ORGANIZATION REPORT NUMBER(S)	5. MONITORING ORGANIZATION REPORT NUMBER(S)
TGAL-TR-83-5	

6a. NAME OF PERFORMING ORGANIZATION	6b. OFFICE SYMBOL (If applicable)	7a. NAME OF MONITORING ORGANIZATION
TELEDYNE GEOTECH Alexandria Laboratories		AFTAC/TG
6c. ADDRESS (City, State and ZIP Code)		7b. ADDRESS (City, State and ZIP Code)
314 Montgomery Street Alexandria, Virginia 22314		Patrick Air Force Base Florida 32925

8a. NAME OF FUNDING/SPONSORING ORGANIZATION	8b. OFFICE SYMBOL (If applicable)	9. PROCUREMENT INSTRUMENT IDENTIFICATION NUMBER
DARPA		F08606-79-C-0007

8c. ADDRESS (City, State and ZIP Code)	10. SOURCE OF FUNDING NOS			
	PROGRAM ELEMENT NO	PROJECT NO	TASK NO	WORK UNIT NO
1400 Wilson Boulevard Arlington, Virginia 22209				

11. TITLE (Include Security Classification)				
(See Block 16)		VT/0709		

12. PERSONAL AUTHOR(S)
R. R. Blandford, J. Goncz, R. Baumstark, K. L. McLaughlin

13a. TYPE OF REPORT	13b. TIME COVERED	14. DATE OF REPORT (Yr., Mo., Day)	15. PAGE COUNT
Technical	FROM 7/24/79 TO 1/10/83	October 30, 1983	92

16. SUPPLEMENTARY NOTATION
EVALUATION OF THE RSTN NETWORK AND FURTHER IMPROVEMENTS TO AUTOMATIC ASSOCIATION

17.	COSATI CODES		18. SUBJECT TERMS (Continue on reverse if necessary and identify by block number)
FIELD	GROUP	SUB. GR.	RSTN, Detection, Threshold, m_b, Lg, LR, Automatic Association, pP, Earthquake Location
08	11		

19. ABSTRACT (Continue on reverse if necessary and identify by block number)

A review of 9 North American events was used to evaluate available RSTN data at the CSS. Signal-to-noise ratios in the time and frequency domains were used to estimate detection thresholds for P, Lg and L_R at regional distances. The P detection threshold at $\Delta \sim 10°$ is near $M_L = 3$. L_g detection thresholds were found to be lower than the P detection thresholds for distances greater than 15 degrees by approximately 0.5 M_L. LR detection thresholds are nearly flat near $M_L \sim 3.5$ for $\Delta \sim 30°$. Due to the small number of events examined, these results are preliminary estimates of detection thresholds. Additional work should investigate the actual detection of small events at regional distances using a larger data base and automated techniques.

20. DISTRIBUTION/AVAILABILITY OF ABSTRACT	21. ABSTRACT SECURITY CLASSIFICATION	
UNCLASSIFIED/UNLIMITED ☒ SAME AS RPT ☐ DTIC USERS ☐	Unclassified	
22a. NAME OF RESPONSIBLE INDIVIDUAL	22b. TELEPHONE NUMBER (Include Area Code)	22c. OFFICE SYMBOL
1Lt Kenneth M. Ols	305-494-5263	TGR

DD FORM 1473, 83 APR   EDITION OF 1 JAN 73 IS OBSOLETE

19) Continued

Further improvements to Automatic Association, AA, have been made to incorporate amplitude data, two array event location, depth phase constraints, unassociated arrivals, and confidence ellipsoids. Two event array location, unassociated arrivals and confidence ellipsoids are completed and help to improve the usefulness and readability of the summary event bulletin. Work on depth phase constraints was evaluated with synthethic arrival date and needs further investigation with real data. Incorporation of amplitude data yields a maximum likelihood estimate of m_b and helps to define a good event and to reject spurious events. It requires more station information (diurnal noise, m_b bias) than is available for many seismic recording systems, however. Its utilization requires that this information be included for each seismic network that AA is applied to.

ABSTRACT

A review of 9 North American events was used to evaluate available RSTN data at the CSS. Signal-to-noise ratios in the time and frequency domains were used to estimate detection thresholds for P, Lg and L_R at regional distances. The P detection threshold at $\Delta \sim 10°$ is near $M_L = 3$. L_g detection thresholds were found to be lower than the P detection thresholds for distances greater than 15 degrees by approximately 0.5 M_L. LR detection thresholds are nearly flat near $M_L \sim 3.5$ for $\Delta < 30°$. Due to the small number of events examined, these results are preliminary estimates of detection thresholds. Additional work should investigate the actual detection of small events at regional distances using a larger data base and automated techniques.

Further improvements to Automatic Association, AA, have been made to incorporate amplitude data, two array event location, depth phase constraints, unassociated arrivals, and confidence ellipsoids. Two event array location, unassociated arrivals and confidence ellipsoids are completed and help to improve the usefulness and readability of the summary event bulletin. Work on depth phase constraints was evaluated with synthethic arrival data and needs further investigation with real data. Incorporation of amplitude data yields a maximum likelihood estimate of m_b and helps to define a good event and to reject spurious events. It requires more station information (diurnal noise, m_b bias) than is available for many seismic recording systems, however. Its utilization requires that this information be included for each seismic network that AA is applied to.

Accession For

NTIS GRA&I	☒
DTIC TAB	☐
Unannounced	☐
Justification	

By____
Distribution/____
Availability Codes

Dist	Avail and/or Special
A-1	

(THIS PAGE INTENTIONALLY LEFT BLANK)

TABLE OF CONTENTS

LIST OF FIGURES

LIST OF FIGURES (Continued)

LIST OF TABLES

(THIS PAGE INTENTIONALLY LEFT BLANK)

EVALUATION OF THE RSTN NETWORK

Introduction

The Regional Seismic Test Network (RSTN) is a 5-station seismic
network designed to monitor regional seismicity on the scale of a large
continental shield. The RSTN serves as a prototype for a network that
could be deployed for test ban treaty verification. Both regional and
teleseismic signals are digitally recorded for three components of earth
motion in three overlapping frequency bands covering 0.02 to 10 Hz.
The instruments, signal conditioning, and recording facilities are
discussed in Rodgers and Hammel (1981), and Breding (1982).

Each station consists of a three component broadband Teledyne
Geotech KS-36000 and a high frequency Teledyne Geotech S-750 in a
borehole at a depth of 100 meters. The KS-36000 output signals are
processed to yield a long period band, an intermediate period band, and
a short period band (see Figure 1). The digital data is transmitted by
satellite to the System Control and Receiving Station in Albequerque, N.
M. (SCARS), and the Center for Seismic Studies (CSS) in Arlington, Va.,
as well as other sites in North America. The data used in this report
was partly received at CSS and partly recorded at SCARS. A description
of RSTN station localities is contained in Taylor and Qualheim (1983).
All RSTN stations are located on Precambrian or Paleozoic sediment at
"hard rock" sites of the Canadian Shield. The network spans nearly 27°
of latitude and 40° of longitude (Figure 2).

Because the RSTN is a sparse network of three-component "broadband"
stations it poses unique problems in the task of developing a regional
system of automatic detection and association. The P_n, Pg, Sn, Lg
regional phases have not been incorporated into a detection, location,
and association process. Three-component stations with three frequency
bandwidths offer the opportunity to determine the optimal frequency
bands for detection and identification of these phases. Regional
detection becomes substantially important in the context of a CTBT
because of agreements between the USA and USSR that internal 3-component
stations could be implemented in the event of such a treaty.
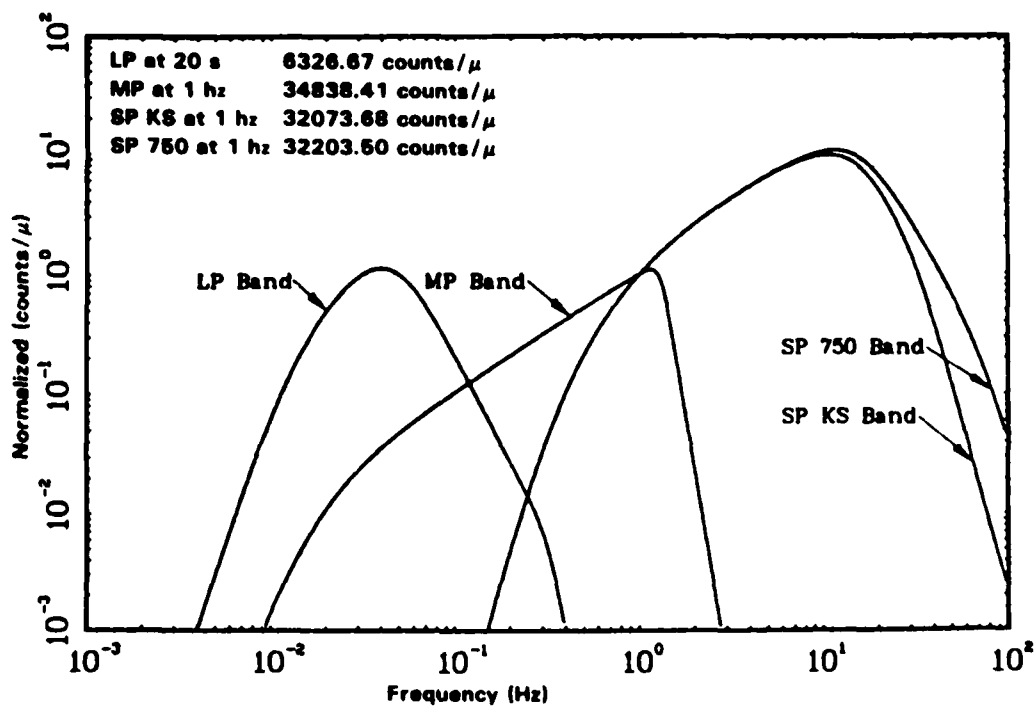
Figure 2.7 RSTN Normalized Displacement Amplitude Responses

Figure 1   RSTN Normalized displacement response from Breding (1982)
            LP: long period band recording
            MP: middle period band recording
            SPK: short period band KS-36000 recording
            SP7: short period band S-750 recording
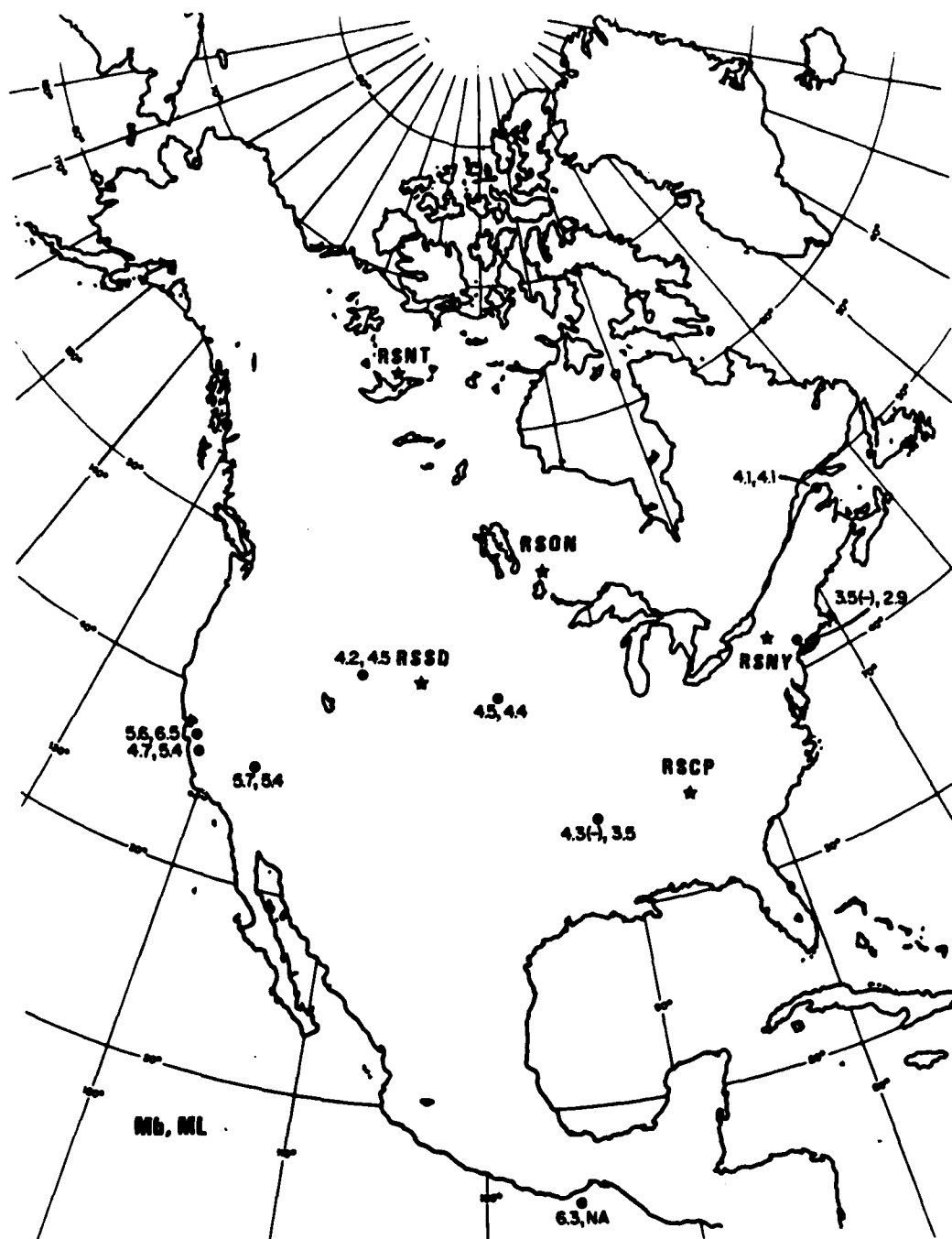
Figure 2 Location of events examined in this report (see Table I) and RSTN station locations M_B and M_L are shown for each event.

TABLE I

Event Location

	M_L	NAME	#	LAT(N)	LON(W)	OT	DATE	M_B
	5.4	NTS	1	37	116	14:00	82/217	5.7
	5.4	CALONE	2	36.3	120.5	22:26	82/298	4.7
	3.5	ARK	3	35.1	92.2	02:30	83/019	4.3
	4.5	YELLOW	4	44.5	110.6	20.25	83/037	4.2
	6.5	CAL	5	36.2	120.3	23:42	83/122	5.6
	4.1	GASPE	6	49.1	67.0	19:35	83/017	4.1
	2.9	NY	7	41.5	73.6	19:59	83/057	3.5
(M_B)	6.3	MEX	8	16.1	95.2	08:17	83/024	5.7
	4.4	DAKOTA	9	44.2	99.4	06:32	83/065	4.5

TABLE II

RSTN Station Locations

RSTN	Lat	Long	Elev
RSNY (New York)	44°32'54"N	74°31'48"W	457m
RSCP (Cumberland Plateau)	35°36'00"N	85°34'08"W	581m
RSSD (South Dakota)	44°07'13.5"N	104°02'10.3"W	2060m
RSON (Ontario)	50°51'32"N	93°42'08"W	405m
RSNT (North West Territories)	62°28'47"N	114°35'30"W	191m

The approach of this study was to select 9 events recorded by the
network and manually analyze the recordings using available software at
the CSS (Table I, and Figure 2). Various phases were identified and
"picked" as well as possible, back azimuths were estimated, and
signal-to-noise ratios were determined. Finally, detection thresholds
as a function of distance were estimated for P, Lg and L_R phases using
the signal-to-noise ratios of the 9 events. Several existing CSS
software packages were tested using the RSTN evaluation data. In the
course of data analysis the quality of RSTN data was examined. Due to
deficiencies in both data quality and available software, some intended
tasks could not be performed on the RSTN data. These tasks were subject
to the programming and computational priorities of the CSS activities.
Data analysis was supported with programs described in Lincoln Lab
manual 132 and standard UNIX software. Several "bugs" were found and
corrected in the existing software. Also, short digital "drop-outs"
detected in the data required additional changes to the existing
software to locate and correct the data drop-outs.

Data Analysis

The following discussion serves to illustrate the analysis performed at the CSS with examples from the RSTN data used in this report.

Figure 3 shows the NTS event, day 217 of 1982, recorded at RSSD. The distance is 11.49°. From top-to-bottom are 40 seconds of three-component short period data, 375 seconds of three-component middle period data, and 1500 seconds of long period data. The P wave is emergent on the short period components with strong radial polarization. The measured apparent azimuth from the horizontal components is within 2 degrees of the computed back azimuth to the event. Lg is clearly visible on the middle period band and L_R is well recorded on the long period band. Although the P arrival is well recorded on the middle period band, the P wave train is not detectable in the time domain on the long period band. The time windows used for spectral estimation of the P wave are indicated with vertical bars labeled "start" and "end". Amplitude signal-to-noise ratios (S/N) were estimated in the time domain and in the frequency domain. The results are tabulated in Appendix I for each event, station, and signal channel. The time domain maximum amplitude S/N was estimated for the short period Z, N, and E components as 98, 73, and 85 respectively. The predominant periods were 0.2, 0.18 and 0.15 seconds on the respective Z, N, and E components.

Figures 4a and 4b are plots of the short period and middle period channel P-wave amplitude spectra for the windows indicated in Figure 3. The noise estimate (dashed line) is computed from a window of the same length for each component directly preceeding the P wave arrival. All spectra in this report are shown as amplitude spectra uncorrected for instrument. The maximum S/N was estimated from each plot as 450, 250, and 525 at 1.1 Hz on the short period band and 466, 350, and 350 at .9 to 1.1 Hz on the middle period band. The long period band P-wave has no significant signal above the noise. The P-wave spectra in Figure 4b are asymptotic to the noise level at 0.2 Hz. This was common at all RSTN stations. A long period explosion P wave null is indicated by the time domain and spectral domain estimates of the P-wave signal strength.

NTS, RSSD
$\triangle° = 11.49$
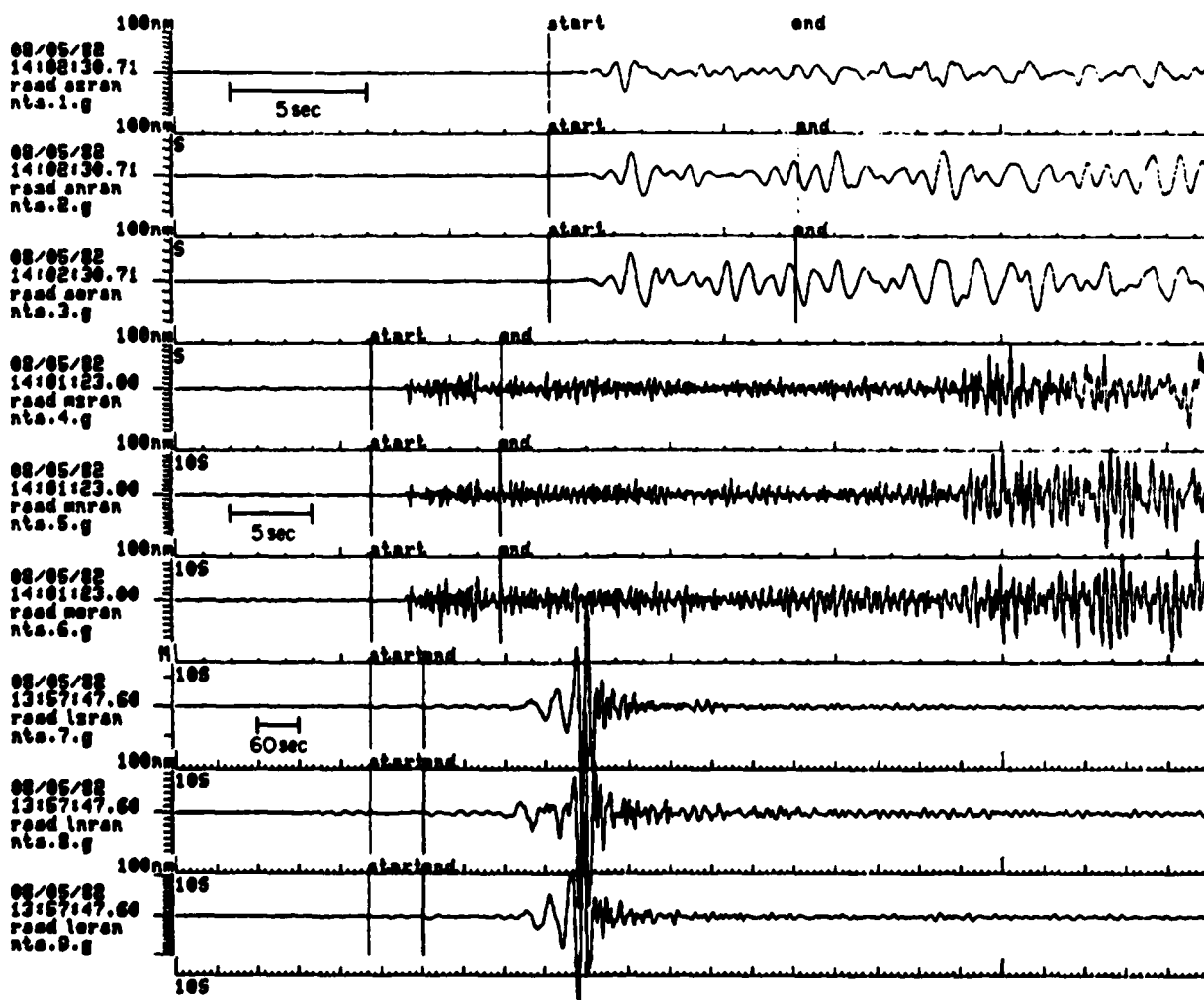
Figure 3   NTS-to-RSSD (11.49°) from top to bottom: Short period Z,N,E
(40 seconds) Mid period Z,N,E (375 seconds) and Long period
Z,N,E (1500 seconds) The vertical scale tick marks are 100nm
for each trace, except the long period Z. The tick marks for
the LPZ are 1 micron increments. The P wave window for
spectral estimation in Figure 4 is shown on each seismogram
indicated by the vertical bars labeled "start" and "end".
Noise windows were selected prior to the P arrival. The P_n
character of P is clear on the short period Z with strong
radial polarization. Lg is clearly observable on the Mid
period band and L_R is well recorded on the long period band.
The P wave is not detectable on the long period.

SPP NTS,RSSD
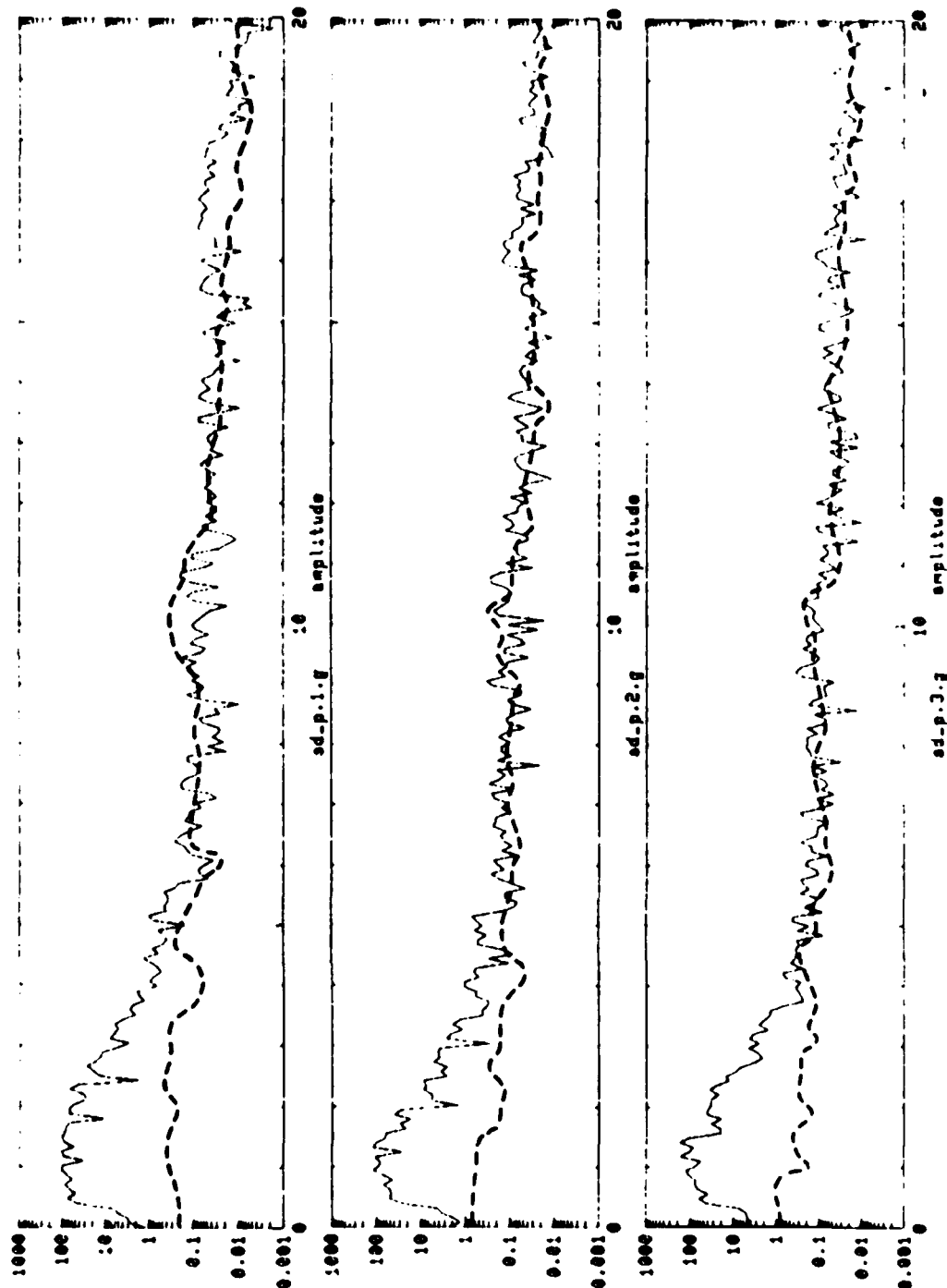
Figure 4A NTS-to-RSSD (11.49°) short period 3-component P wave
amplitude spectra with noise spectra superimposed. Units are
nm-(sec)f/2 at 1 Hz. Spectra are not corrected for frequency
dependent instrument response. Signal-to-noise ratio is
estimated as 450, 250, and 525 on Z, N, E respectively all at
1.1 Hz.

-8-

MPP NTS,RSSD
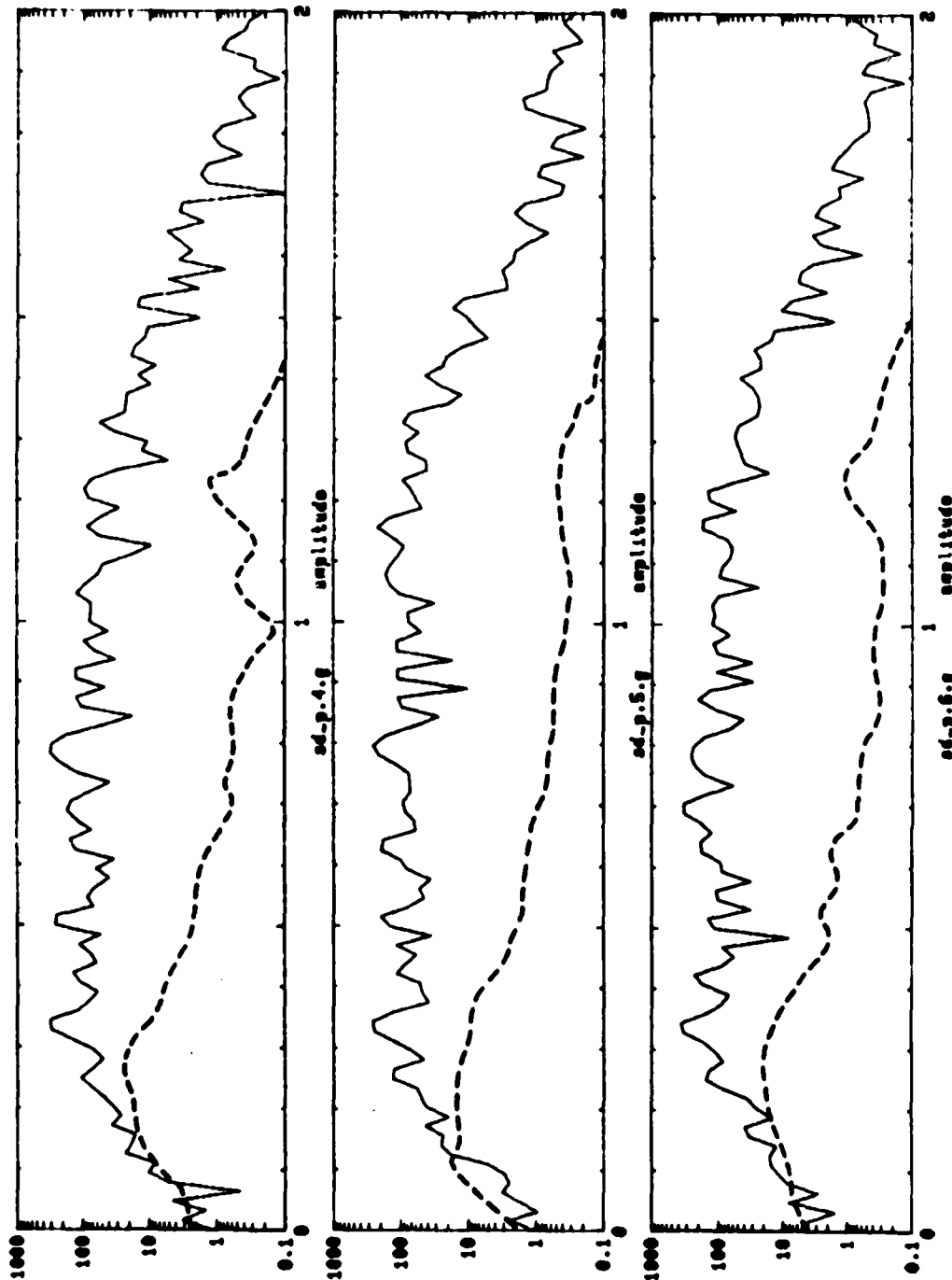
Figure 4B NTS-to-RSSD (11.59°) Mid period 3-component amplitude spectra with noise spectra superimposed. Signal-to-noise is estimated as 566, 350, and 350 on Z,N,E at .98, 1.12, and .9 Hz respectively. Spectra are asymptotic to noise levels at frequencies below 0.20 Hz₁½indicative of a long period P wave null. Units are nm-(sec) at 1 Hz. Spectra are uncorrected for frequency dependent instrument response.

For comparison with the explosion traces of Figure 3, the California earthquake of 10/25/82, M_L 5.4 ($\wedge = 14.78°$), is shown in Figure 5a. The initial short period P-wave appears with much the same signal-to-noise ratio as the NTS event, while the long period P-wave is clearly visible on the bottom three traces. Love and Rayleigh waves are clearly seen on the long period records. S waves are apparent on both middle and long period band records. In Figures 5b and C, P-wave middle period and long period spectra are observed above the noise at frequencies below 0.1 Hz at this distance and magnitude level for earthquakes.

Lg signal-to-noise ratios are estimated in much the same way as P-wave signal-to-noise estimates. Figure 6a demonstrates the short period Lg spectra of the NTS event at RSSD ($\wedge = 11.49°$) and Figure 6b illustrates the same on the middle period band records. Lg has similar amplitudes on all three components of motion. The maximum signal-to-noise ratio for Lg was found at 0.5 to 0.7 Hz on both short period and middle period channels. Similarly, the long period L_R signals are presented in Figure 7.

As an example of a shorter intra-shield propagation path, the Dakota earthquake recorded at RSSD ($\wedge = 3.3°$) is shown in Figure 8. There is a well developed Pg-Pn separation of 8 seconds on the short and middle period bands. Propagation is from the east (87°) and the P wavetrain is best observed on the vertical and east components. S waves and Lg are well developed on the middle period band. A broadband pulse of superimposed S and surface waves is prominent on the long period records.

In contrast to the NTS P-wave spectra at RSSD (Figure 4a) the spectra of the Dakota earthquake in Figures 9a and b are above the noise to the Nyquist frequencies at 20 Hz and 2 Hz. Some aliasing may be present.

At this point we should point out some aspects of the short-period noise spectra. In Figures 4a and 6a the "noise" spectra are all nearly flat between 6 and 10 Hz. This is common for RSSD. Between 10 and 20 Hz the level declines to .01 m$_\mu$. The spectra have not been corrected for instrument response and the high frequency level corresponds to a

-10-
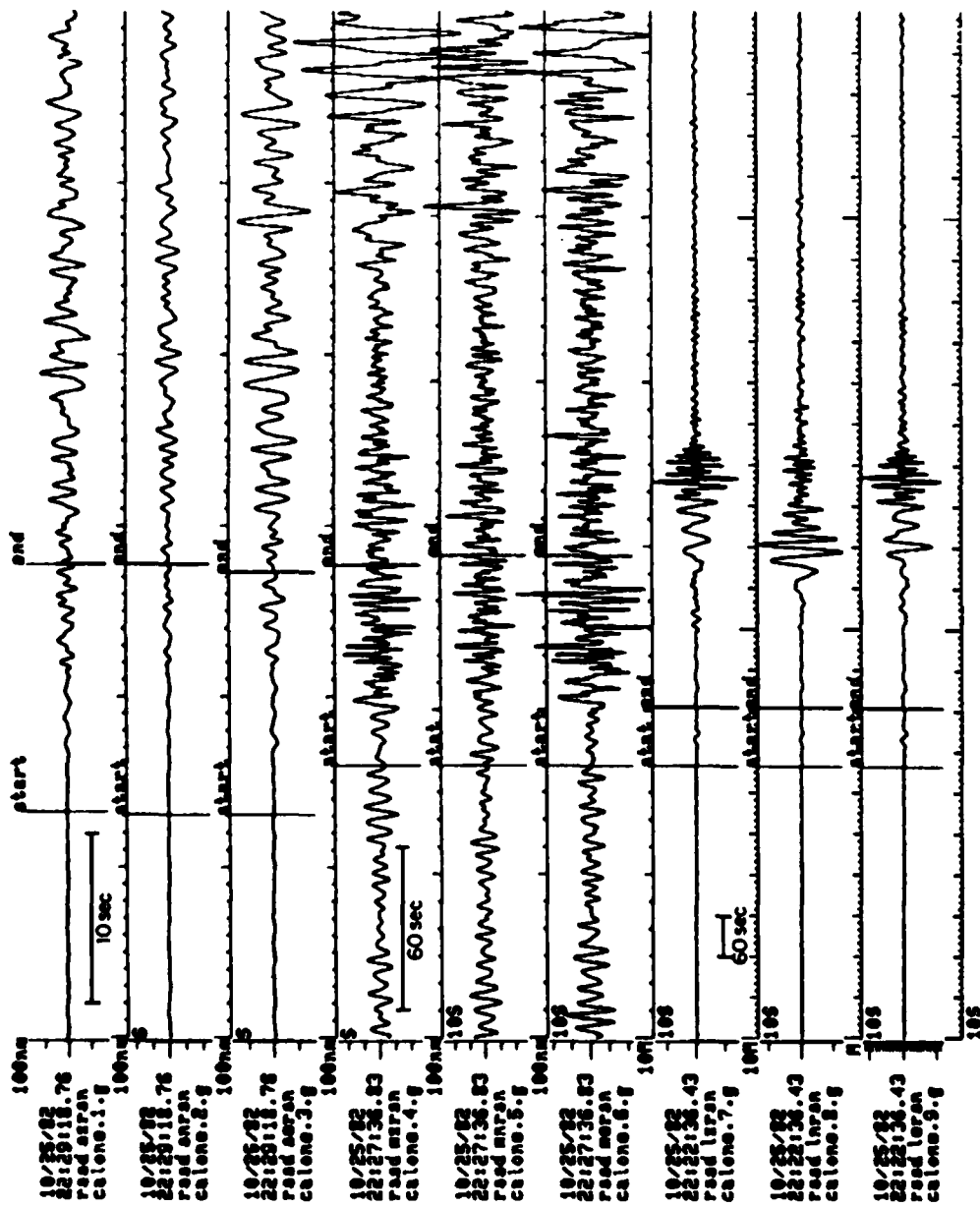
Figure 5A Calone-to-RSSD (14.78°) (Scales same as Figure 3) P wave,
Love and Rayleigh surface waves are the long period records.

MPP CALPONE, RSSD
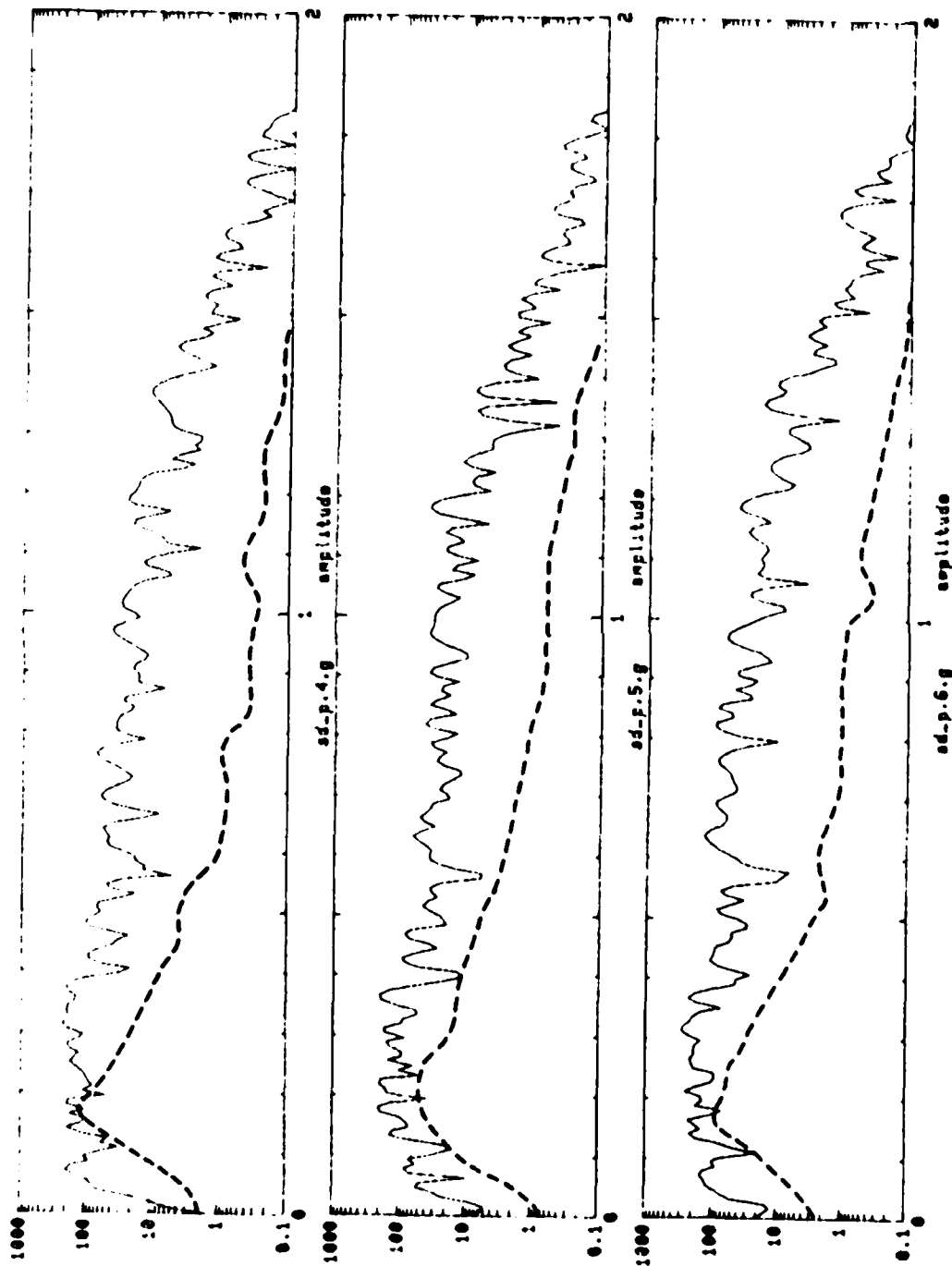
Figure 5B Calone-to-RSSD (14.78°) Mid period P wave amplitude spectra
with noise estimates. P wave spectra remain above the noise
across the microseism band at 0.2 Hz.

LPP CALONE, RSSD
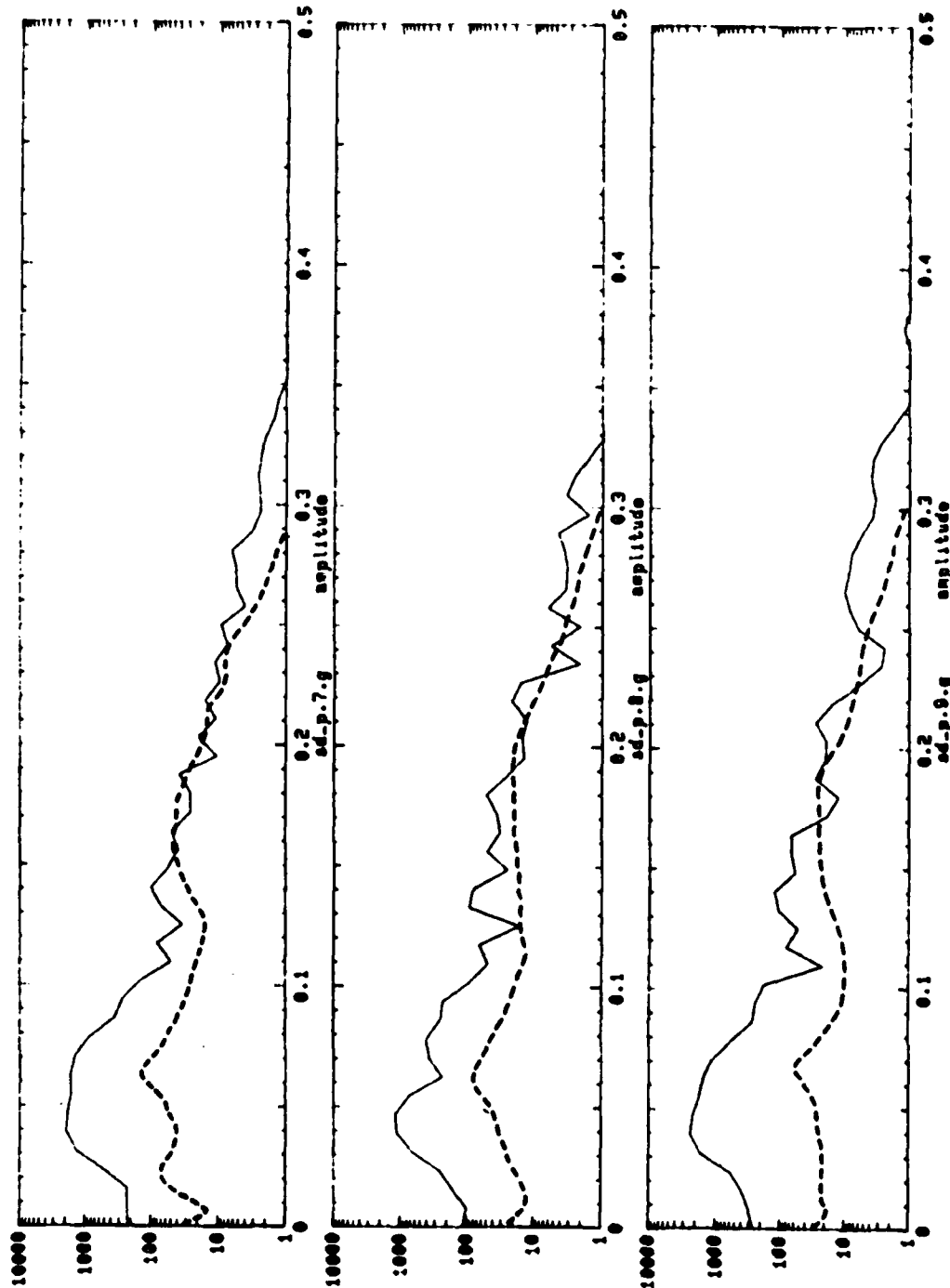
Figure 5C Calone-to-RSSD (14.78°) Long period P wave amplitude spectra
with noise estimates. P wave spectra remain above the noise
at frequencies below 0.1 Hz.

SPLg NTS.RSSD
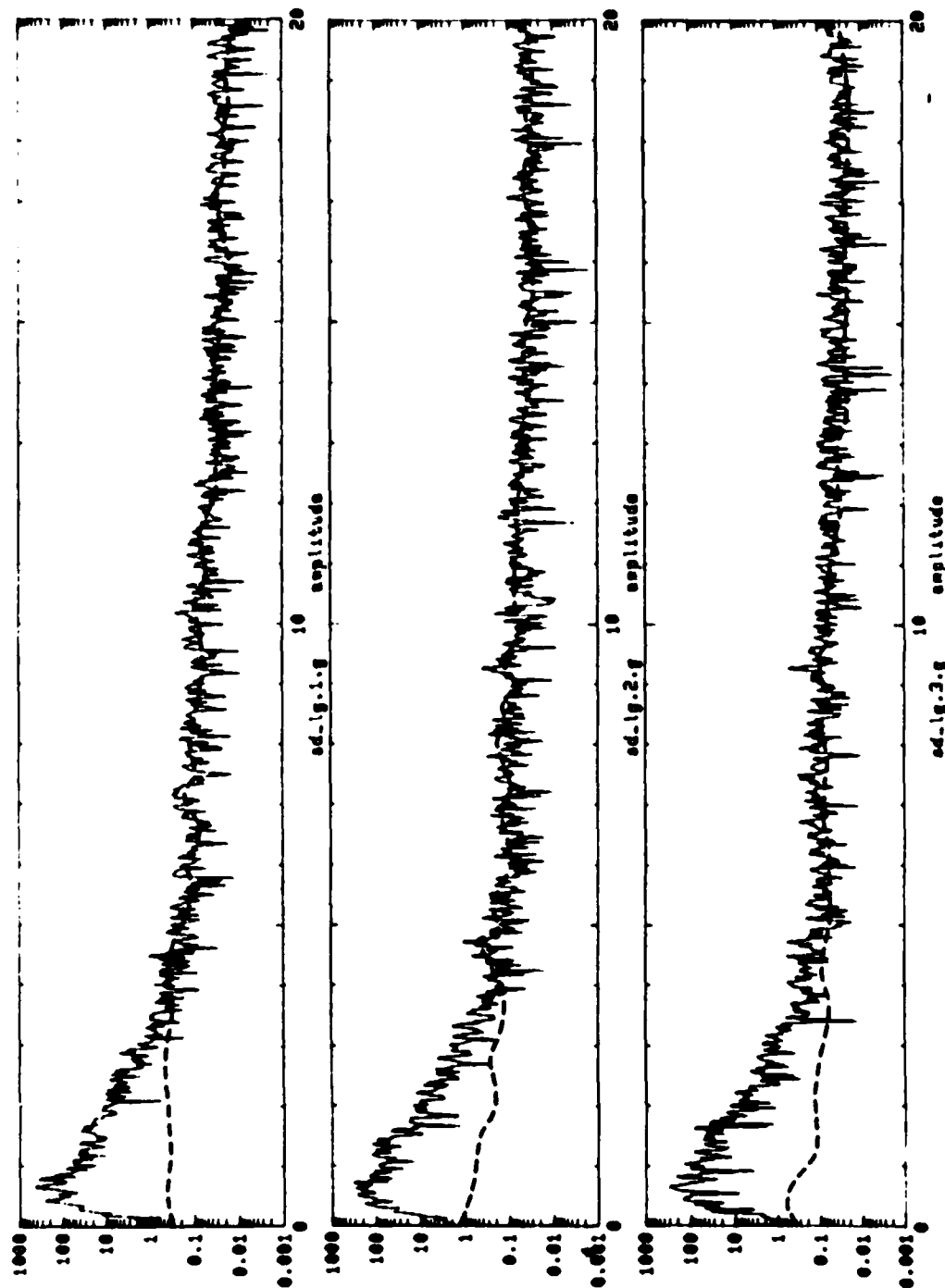
Figure 6A NTS-to-RSSD (11.49°) Short period Lg amplitude spectra with noise estimates. Signal strength is much the same on all three-components. Signal and noise amplitudes are flat at levels near .01 mu above 5 Hz. Maximum S/N estimates for Z, N, and E are 500, 285, and 250 at 0.7, 0.7, and 1.3 Hz respectively.

MP Lg NTS,RSSD
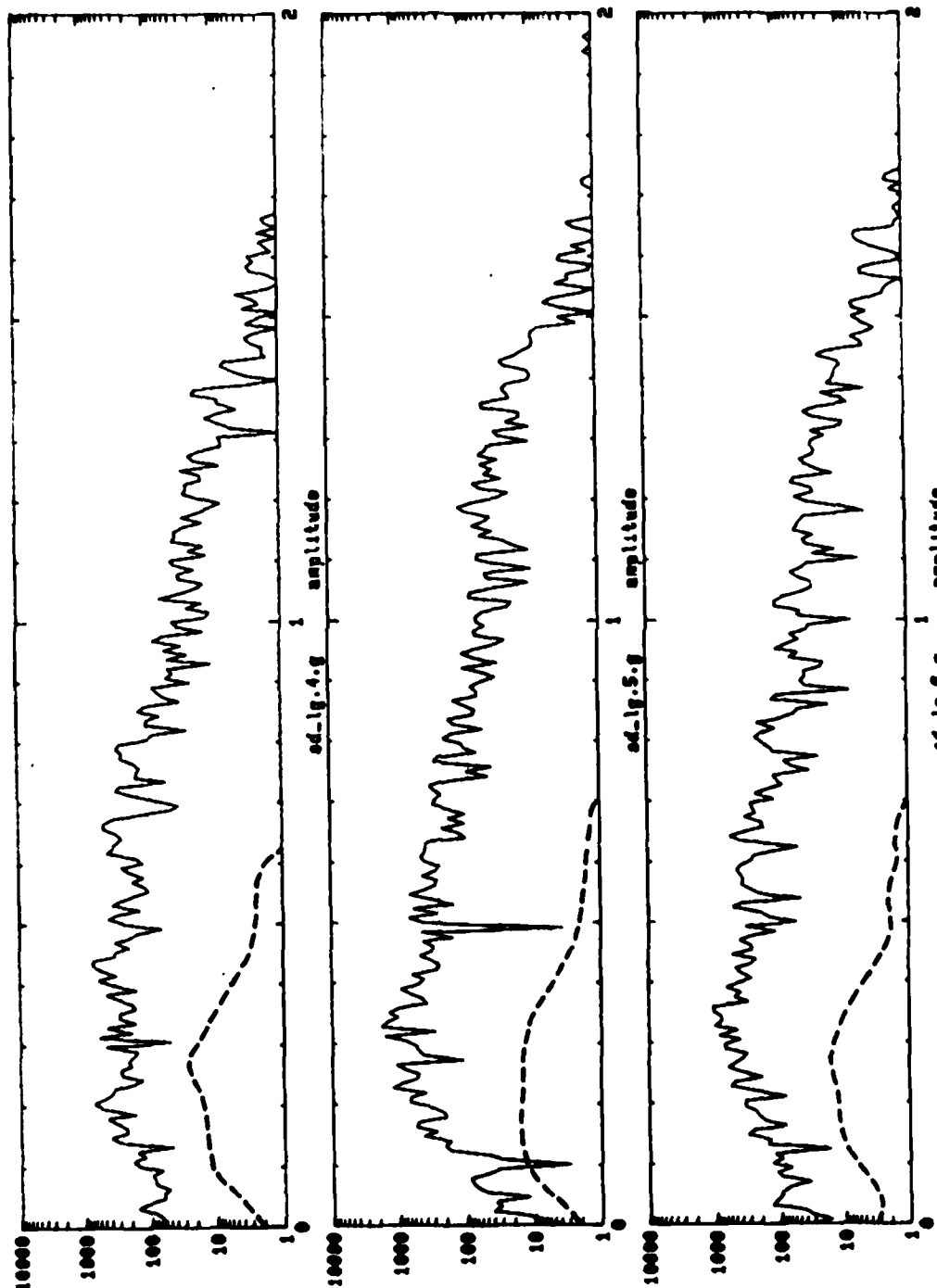
Figure 6B NTS-to-RSSD (11.49°) Mid period Lg amplitude spectra with noise estimates. Maximum signal-to-noise ratios at 511, 200, and 200 at 0.64 0.55 and 0.66 Hz. Lg signal is strong across the microseism band at 0.2-0.3 Hz.

LPLR NTS,RSSD
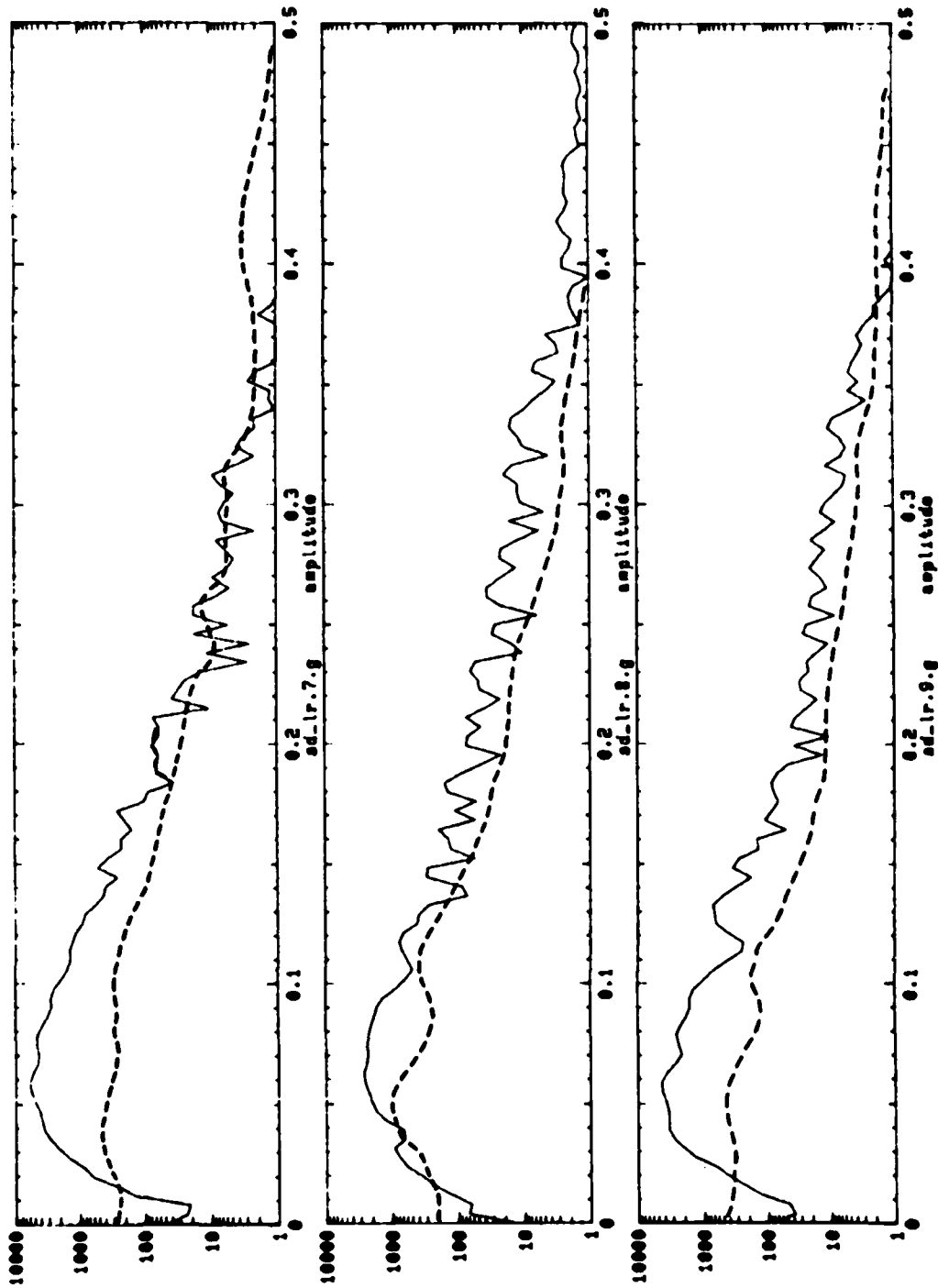
Figure 7   NTS-to-RSSD (11.49°) Long period L_R amplitude spectra with noise.

DAKOTA, RSSD
$\Delta^{\circ} = 3.3$
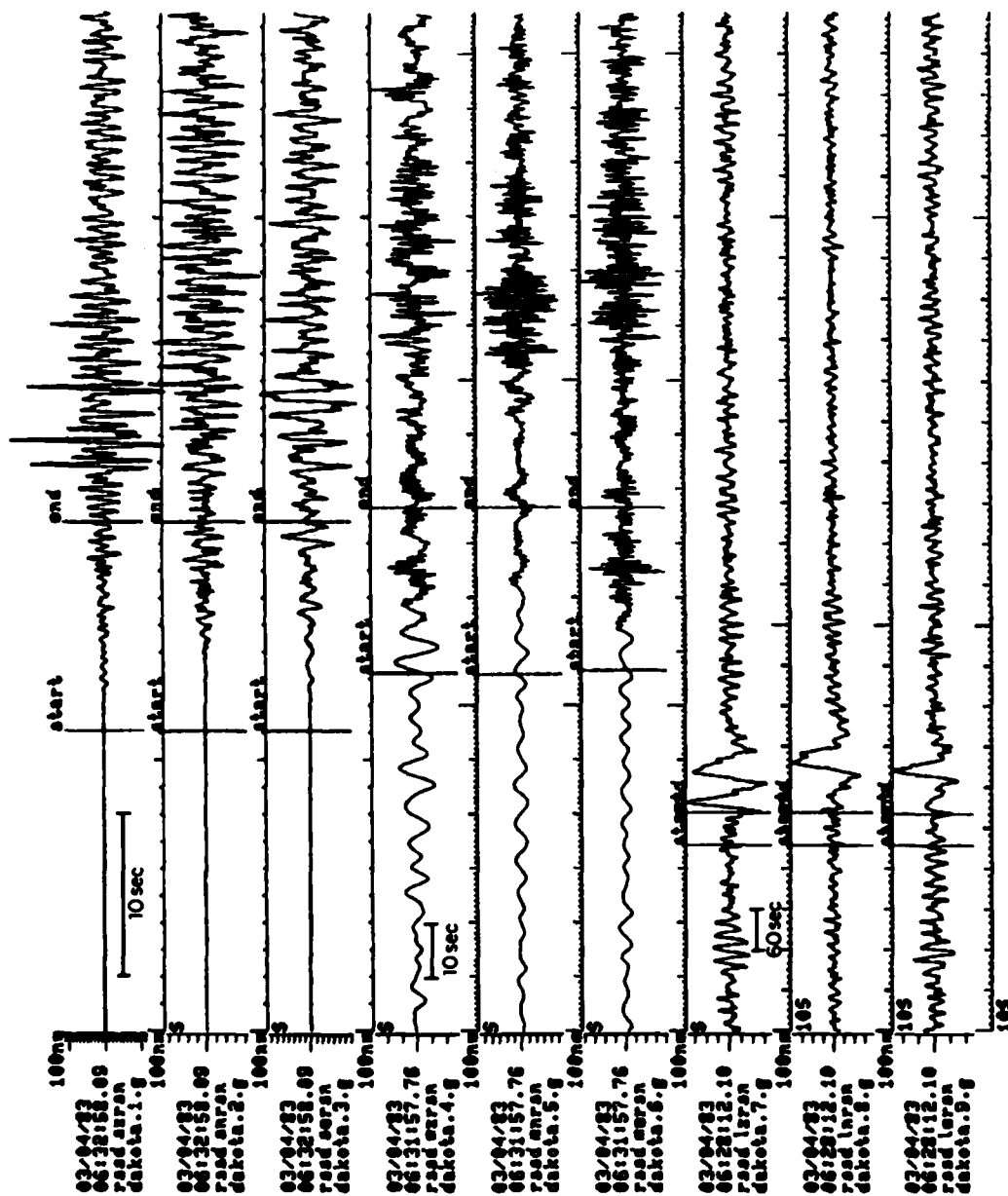
Figure 8   Dakota-to-RSSD (3.3°, M_L 4.4) Near regional event shows well developed P_g-Pg separation of 8 seconds on short period and mid period Z&E. (Azimuth of approach ESE) S waves and Lg are well developed on the mid period band. A Rayleigh pulse is prominent on the long period band.

SPP DAKOTA,RSSD
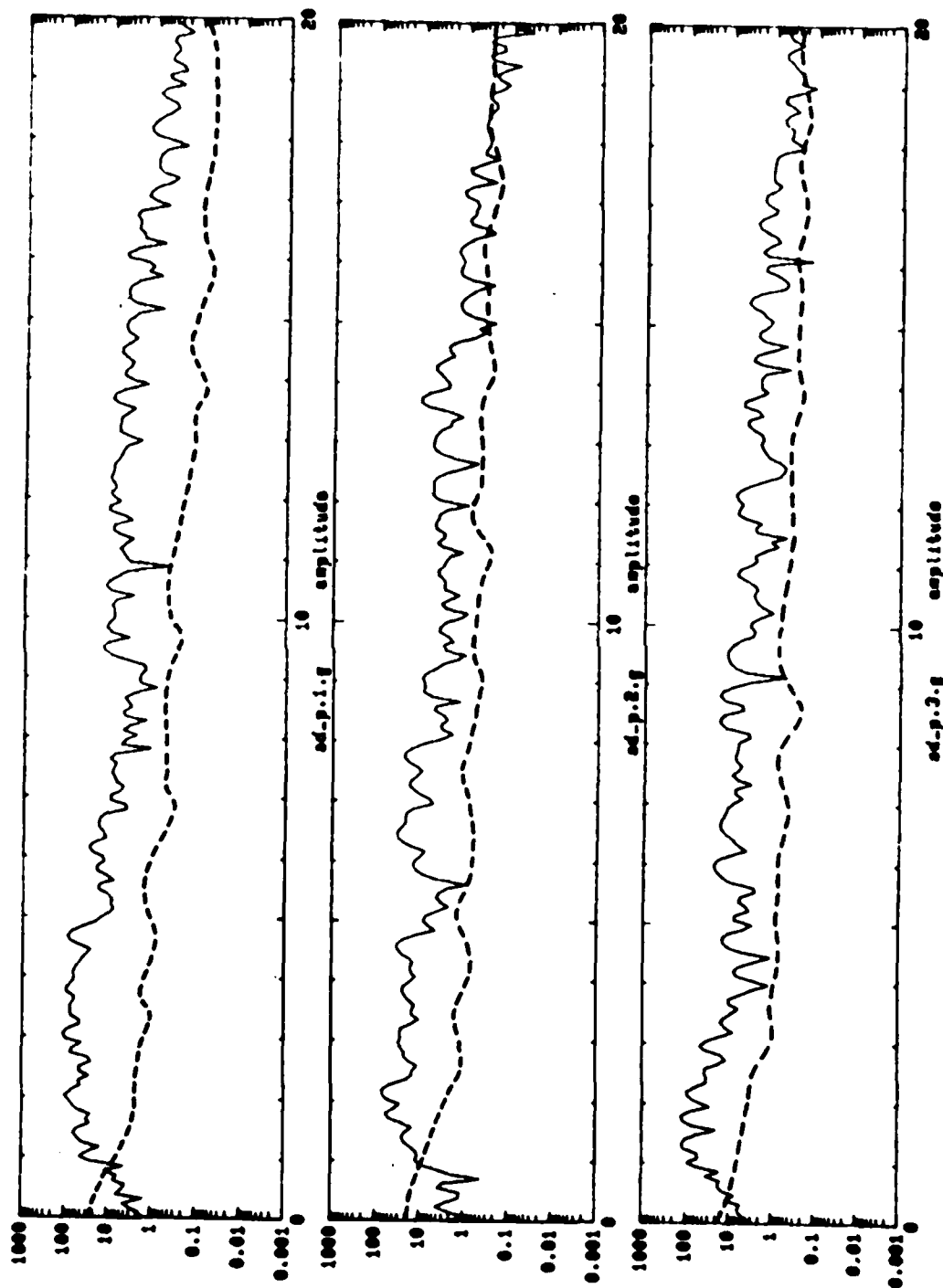
Figure 9A Dakota-to-RSSD (3.3°, M_L 4.4) Short period P wave amplitude spectra with noise levels. P wave spectra above the noise throughout the band width. Signal to noise has multiple local maxima at 3.7 and 13.1 Hz. (Noise estimate is plotted 1 decade too high)
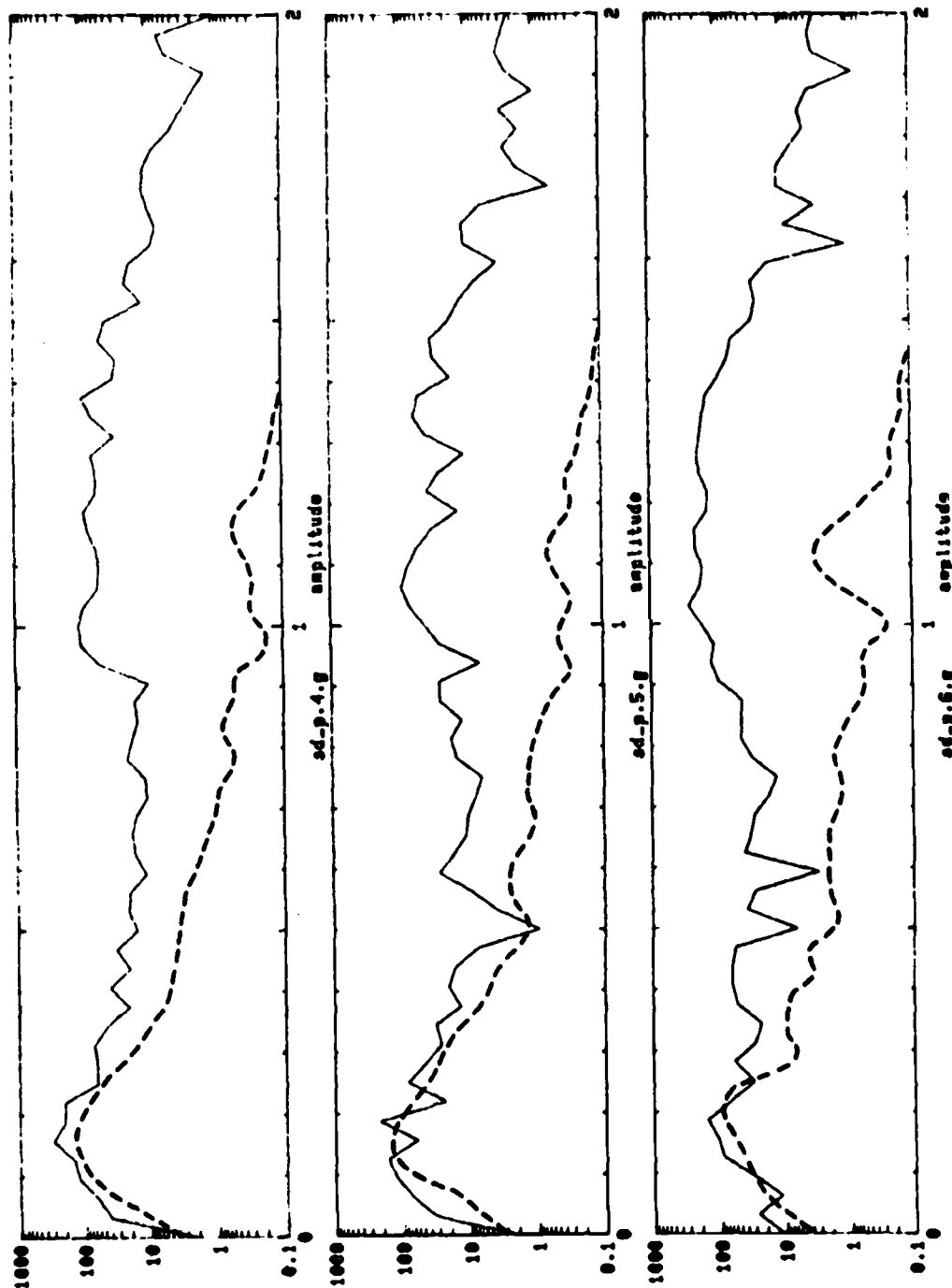
Figure 9B Dakota-to-RSSD (3.3°, M_L 4.4) Mid period P amplitude spectra with maximum signal-to-noise near 3 Hz.

signal level of $\pm.5$ least significant bit (LSB), the quantization level. For the short period band, this corresponds to .01 m $_{\mu}/\sqrt{Hz}$ at the reference frequency of 1.0 Hz. At highest gain, the short-period LSB = 0.031 m μ and the effect of quantization noise may be viewed as white noise with rms amplitude of LSB/ $\sqrt{12}$ (Openheim and Schafer, 1975) or 0.01 mμ. At the next lowest gain level the quantization noise level is .07 mμ. For a larger amplitude signal that was predominately recorded at a greater gain level, the quantization noise level will be higher.

Table III summarizes the short-period quantization noise levels at the four gain levels that are used with the automatic gain-ranging. To be precise, the white noise level contribution to the final spectra is a sum of the proportional time periods at each automatic gain level.

The limiting white noise level is at best .01 mμ at 1 Hz. When corrected for instrument response this means that some RSTN short-period recordings are sensing quantization noise and not local ground motion at frequencies above 10 Hz, during quiet time periods (Figure 6a noise levels). Furthermore, the flat signal spectra above their "noise" levels at high frequencies may not be significant since the signals were recorded at a higher gain levels than the ambient "noise" signals. Consequently, it is not clear that the signals observed in Figures 4a, 6a and 9a are at or below ambient noise levels at high frequencies. Previous studies of ambient noise levels at quiet sites (Herrin, 1982; Fix, 1972) indicate that ambient noise levels continue to decline at high frequencies.

The frequency response and gain levels of the RSTN instruments were designed so that the expected ambient ground noise averaged over 1/2 octave bands, was an rms 5 counts up to 10 Hz. The response declines at frequencies above 10 Hz to ensure that aliasing of ground and system noise is unimportant. The model for ambient ground noise was based on known quiet sites such as Lajitas (Herrin, 1982). Recent reports from NORSAR (Bungum, 1983) indicate that southeastern Norway has very similar noise levels at 10 Hz. If these are globally representative noise levels then it is expected that such quiet sites as RSSD will show quantization noise from time to time for frequencies near and above 10 Hz. This is not unexpected given the design criteria of the RSTN response.

TABLE III

Short-period Band Quantization White Noise Contribution at Different
Gain Levels.

Gain Level Indicator	Resolution LSB mμ	RMS White Noise Level mμ
11	3.99	1.15
10	.99	.28
01	.25	.07
00	.031	.01

Estimation of Detection Thresholds

An effort was made to estimate detection thresholds as a function of distance for P, Lg and L_R within the three frequency bands. Figure 10 illustrates the procedure using the NTS (M_L 5.4) event and short period, P-wave and Lg signal-to-noise estimates. The location of the NTS event is shown together with the five RSTN stations. At each station the logarithm (base 10) of the maximum signal-to-noise ratio is shown and the frequency at which it was measured. In the case of RSNY the short period Lg was not detected. In the case of RSCP, the Lg record was not available. The difference between the log(S/N) and the local magnitude provides an estimate of the possible detection threshold. For instance, an estimate of M_L 3.0 is derived for the detection threshold at RSSD for the NTS source area on the short period instrument. A value closer to 5.0 M_L would be indicated for short period Lg. Similarly, Figure 11 presents the short period and long period P-wave signal-to-noise ratios, (S/N), for the Dakota earthquake. Figures 12 and 13 show the (S/N) for the Arkansas and New York earthquakes.

The M_L was used in these analysis where available since it more properly measures the high frequency content of the source than the low frequency measure M_S or the narrow band measure m_b. Because the velocity response of the middle and short-period band recording is flat in the pass bands of interest, the amplitude measurements were not corrected to period; (A) not (A/T) was used in the analysis.

All the estimated short-period detection thresholds are combined in Figure 14 and plotted versus distance. Each estimate is coded acording to event number. If no short period P detection was made an up arrow (↑) indicates the lower limit that is implied by the lack of detection.

The intra-shield paths of events (3) Arkansas, (4) Yellowstone, (6) Gaspe, (7) New York, and (9) South Dakota may have systematically lower thresholds. The non intra-shield paths of (5) NTS, (2) and (5) California, and (8) Mexico could be expected to pose additional attenuation to P-waves. Some of the Lg (S/N) is presented in Figures 15, 16, 17, and 18 together with the L_R (S/N) data. The Lg detection
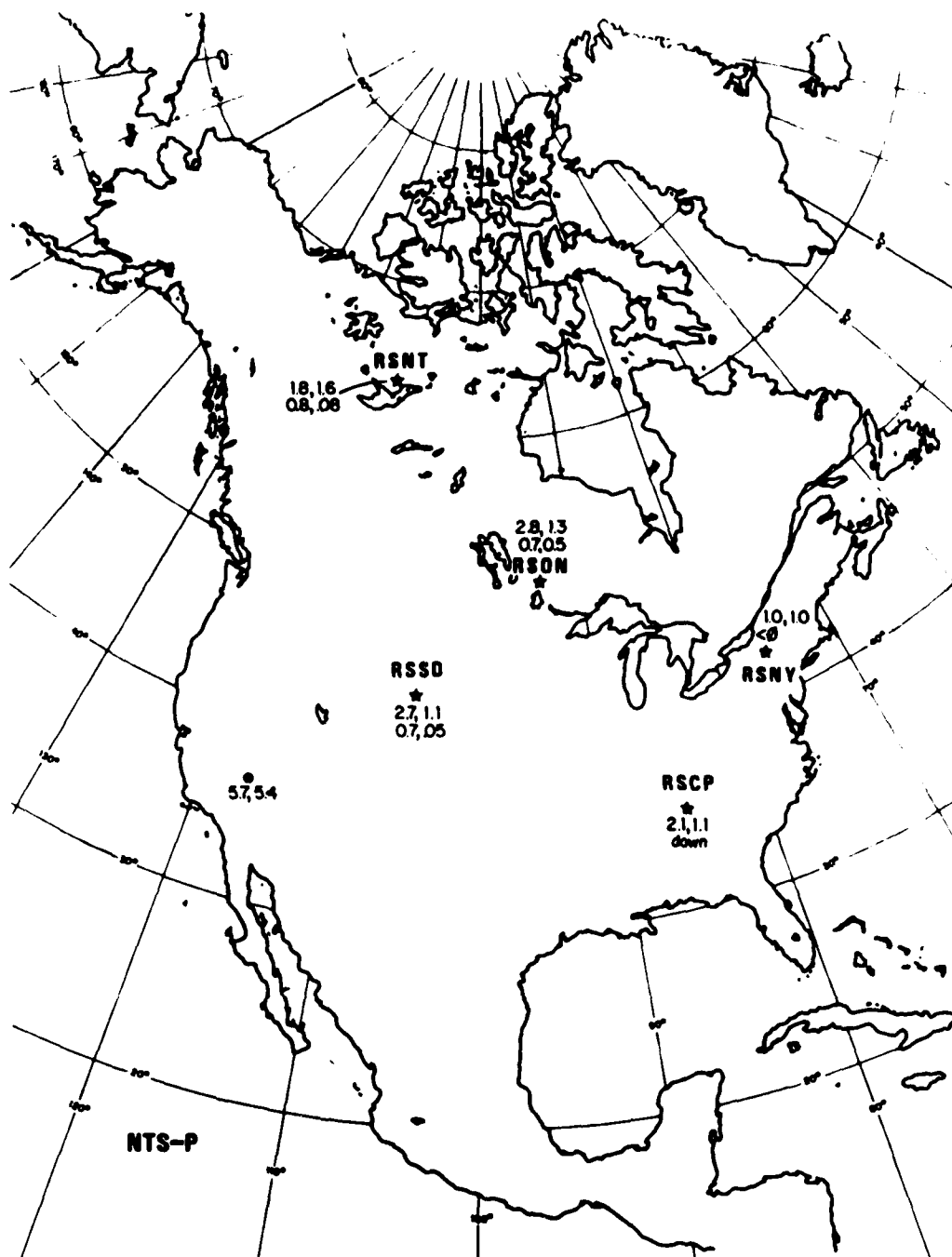
Figure 10   NTS short and long period P wave detection: P logarithmic
maximum signal-to-noise ratios and frequency at which the
maximum signal-to-noise was measured.   The top pair of values
is for short period P and the bottom pair of values is for
long period P.   The M_L 5.7 NTS explosion had a P wave
logarithmic signal-to-noise ratio of 2.7 at 1.1 Hz RSSD
(3.3°).   Similarly the long period P logarithmic
signal-to-noise ratio was 0.7 at 0.34 Hz.   A detection
threshold of M_L 3.0 for this path is indicated for P and M_L
5.0 for long period P.
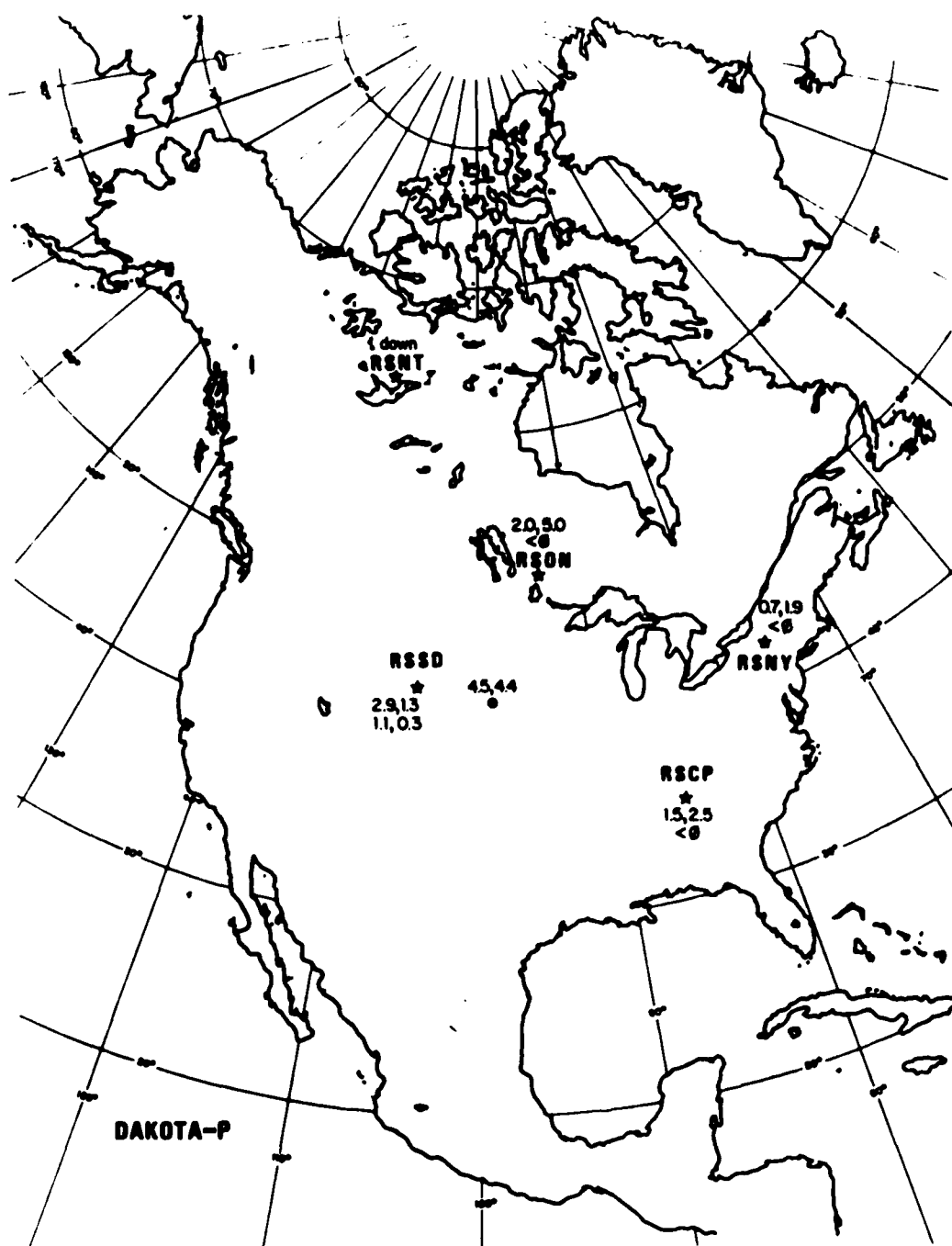
DAKOTA-P

Figure 11 Dakota earthquake (M_b 4.5) short period and long period P
wave detection. RSNT records were not available for this
event, and long period records did not show a P wave for this
event at RSON, RSNY and RSCP (< 0). A logarithmic P wave
signal-to-noise ratios of 0.7 at RSNY indicates that a
detection threshold of 3.8 or better is possible for
intra-shield distances of 17°. Similarly a detection
threshold of 2.5 may be indicated for RSON at 8°.
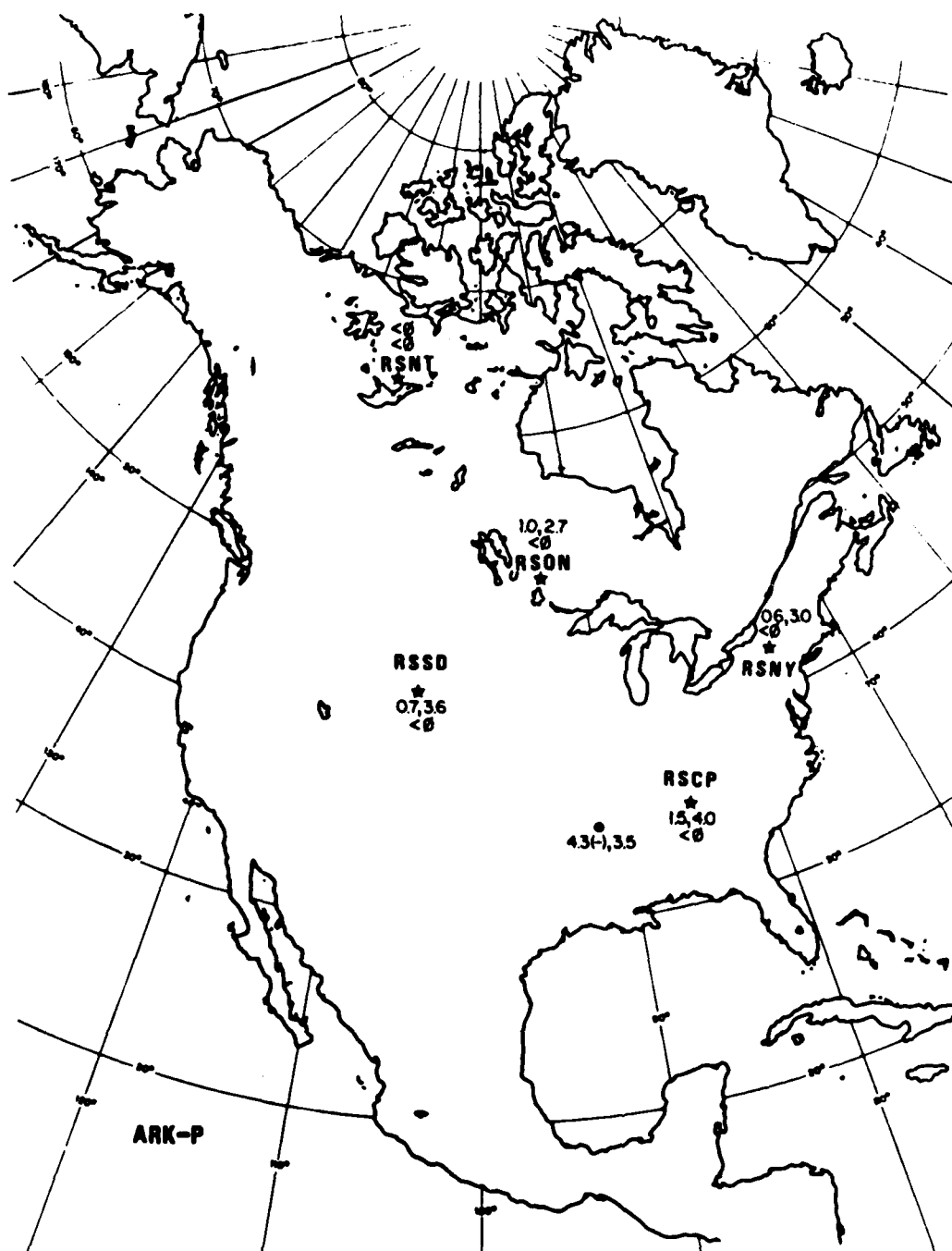
Figure 12 Arkansas earthquake (M_L 3.5) Short and long period P wave
detection and logarithmic signal-to-noise ratios. The event
was below detection threshold at RSNT for both short and long
period P waves and below long period threshold for all
stations. Short period detection threshold of 3.8, 3.7 and
3.3 are indicated for the path to RSCP (5.4°), RSNY (16°) and
RSON (16°) paths.
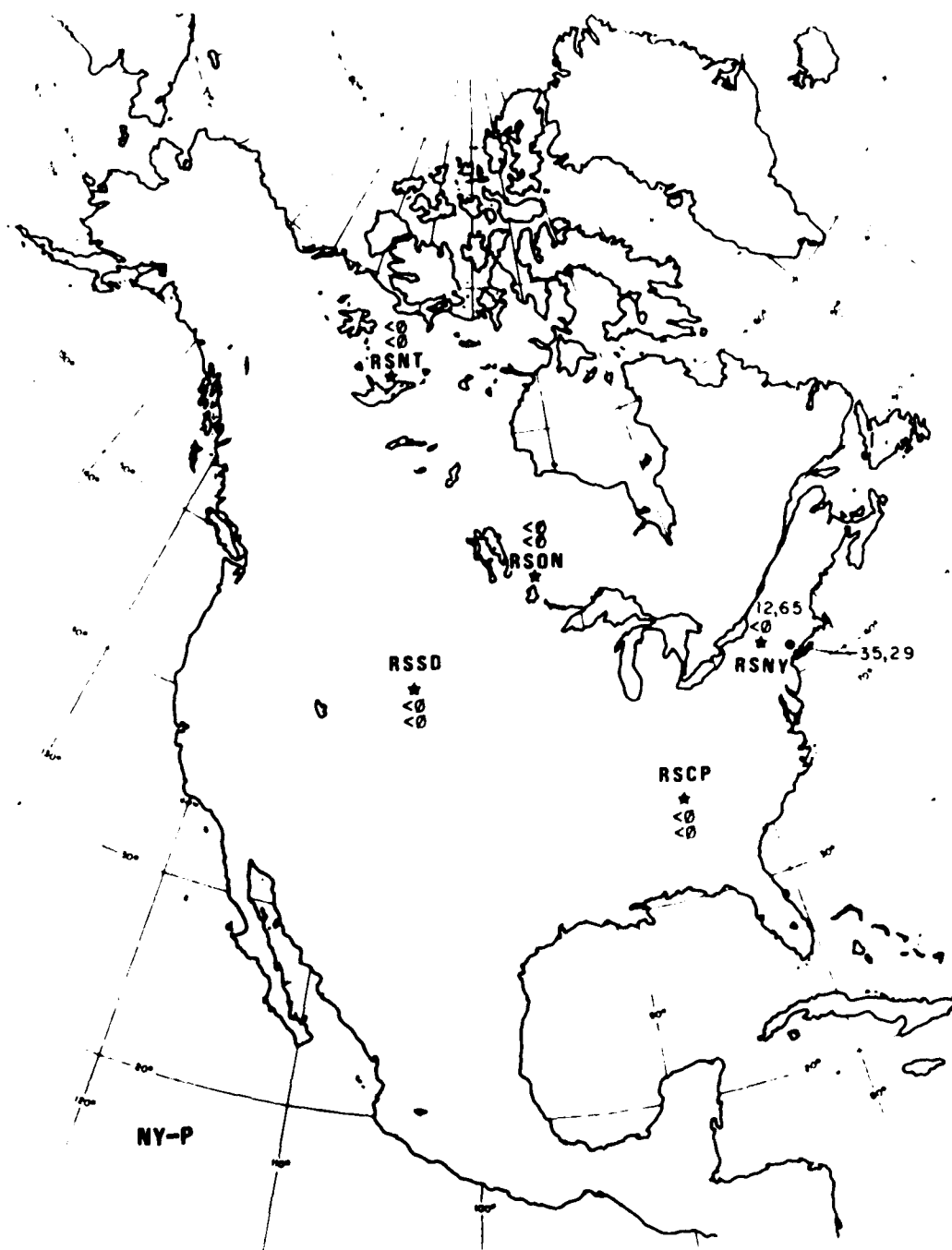
Figure 13   New York earthquake (M_L 2.9) short and long period P wave
detections.
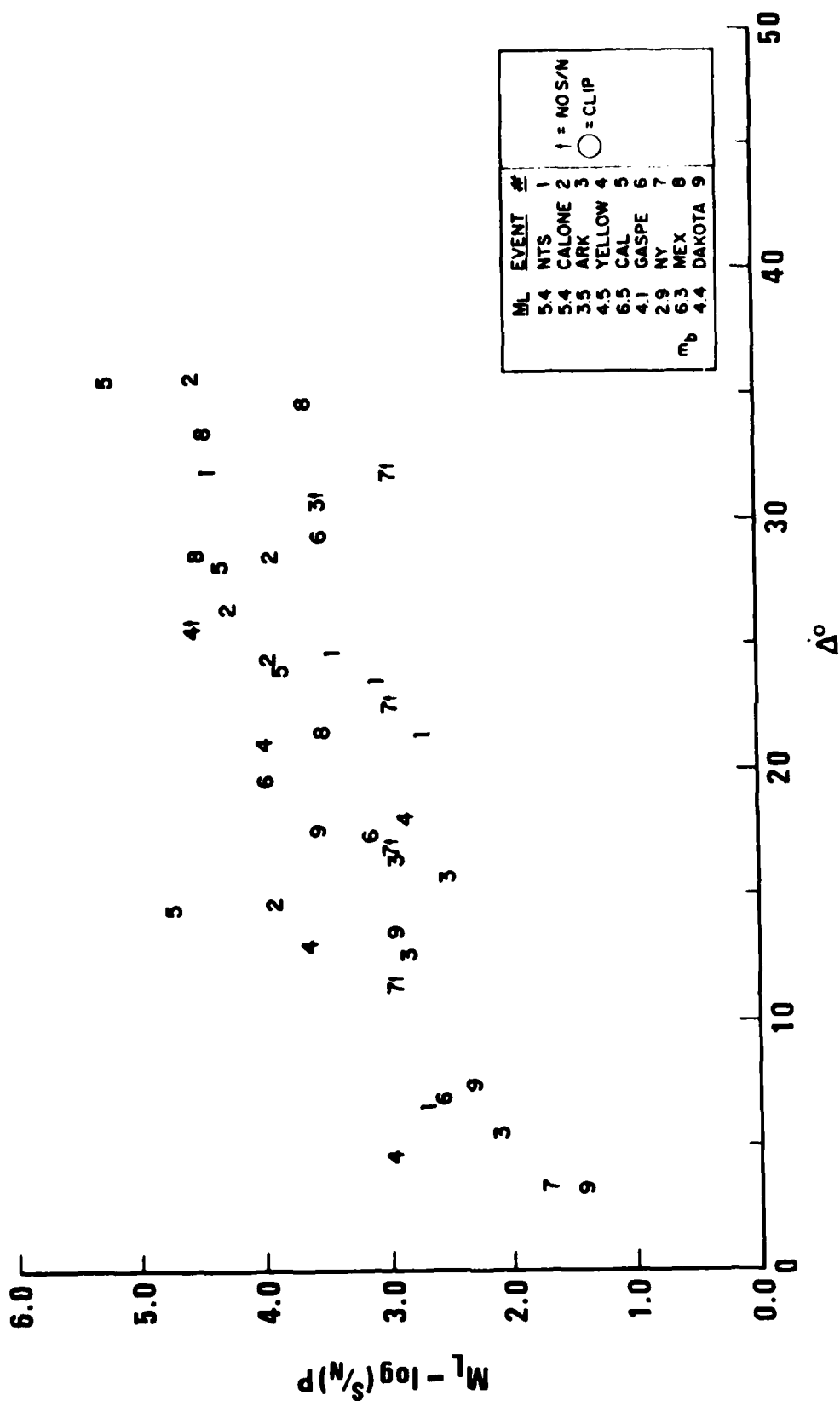
Figure 14 Estimated detection thresholds from short period P
signal-to-noise ratios. No short period P detections are
indicated by †. Non intra-shield paths NTS (5), Calone (2),
CAL (5) and MEX (8) may be systematically higher than
intra-shield paths ARK (3), Yellow (4), GASPE (6), NY (7) and
Dakota (9).
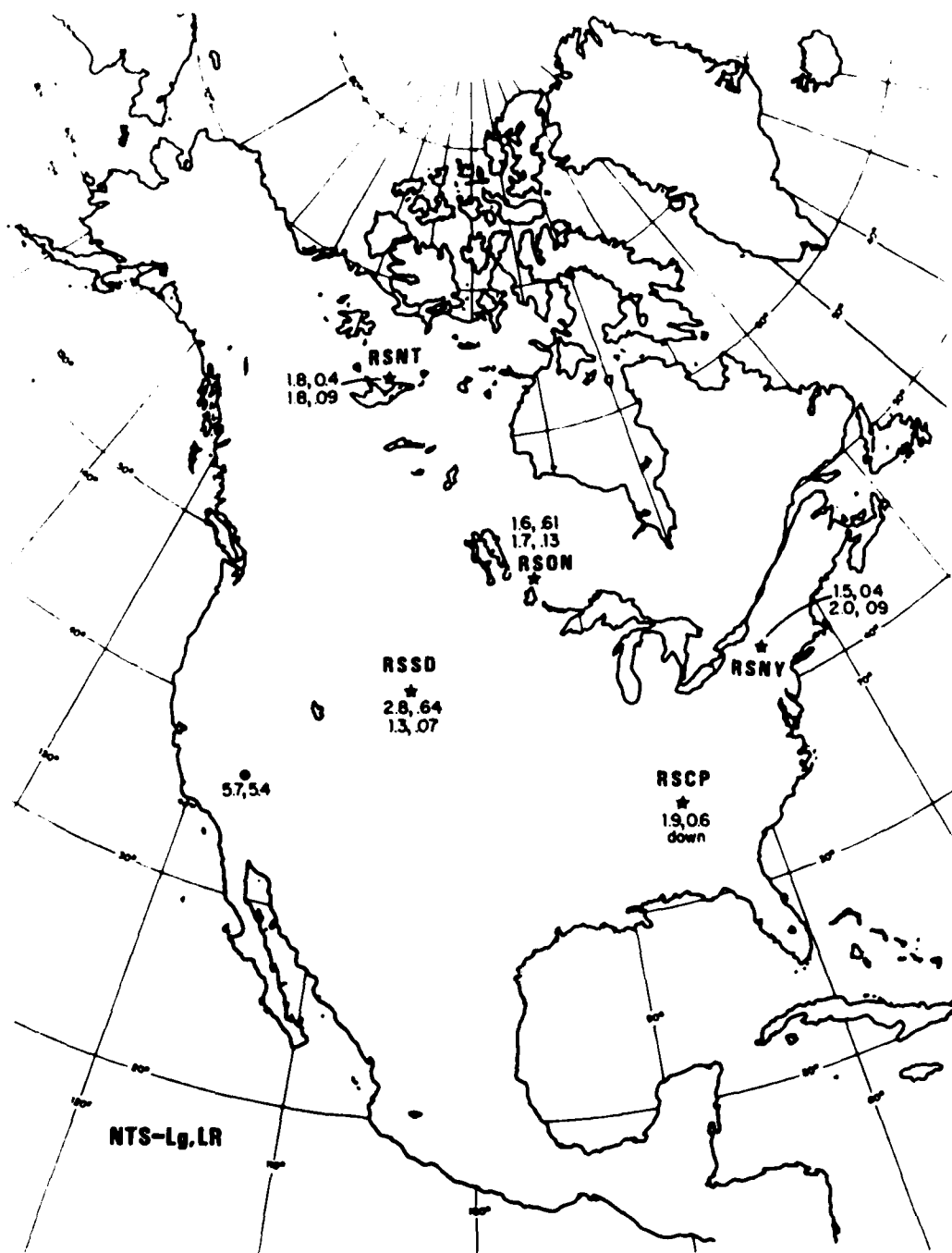
Figure 15   NTS explosion Lg and L_R logarithmic signal-to-noise ratios.
Top pair is logarithmic S/N and frequency for Lg. Bottom
pair is for L_R.
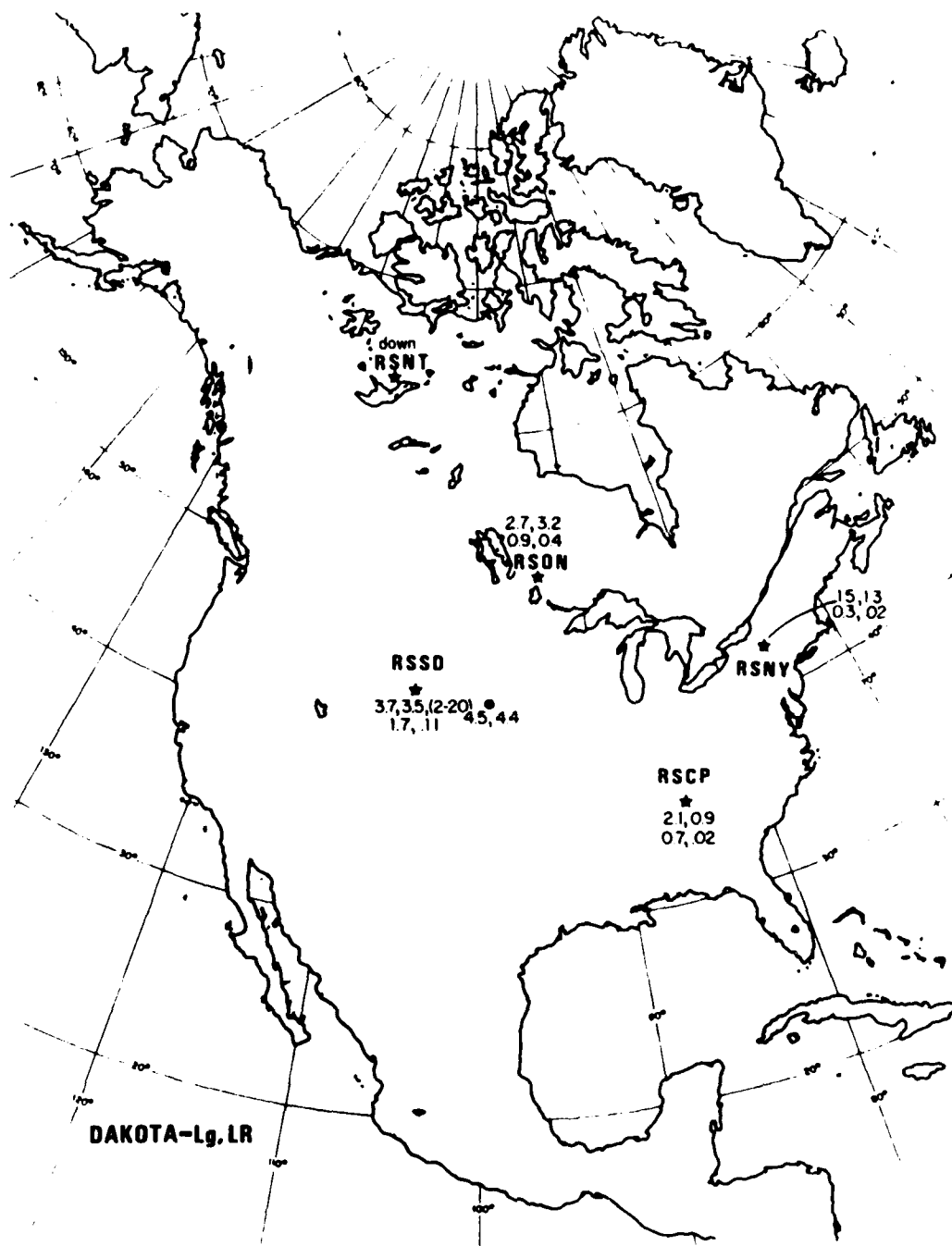
Figure 16   Dakota earthquake Lg and L_R logarithmic signal-to-noise
ratios earthquake.
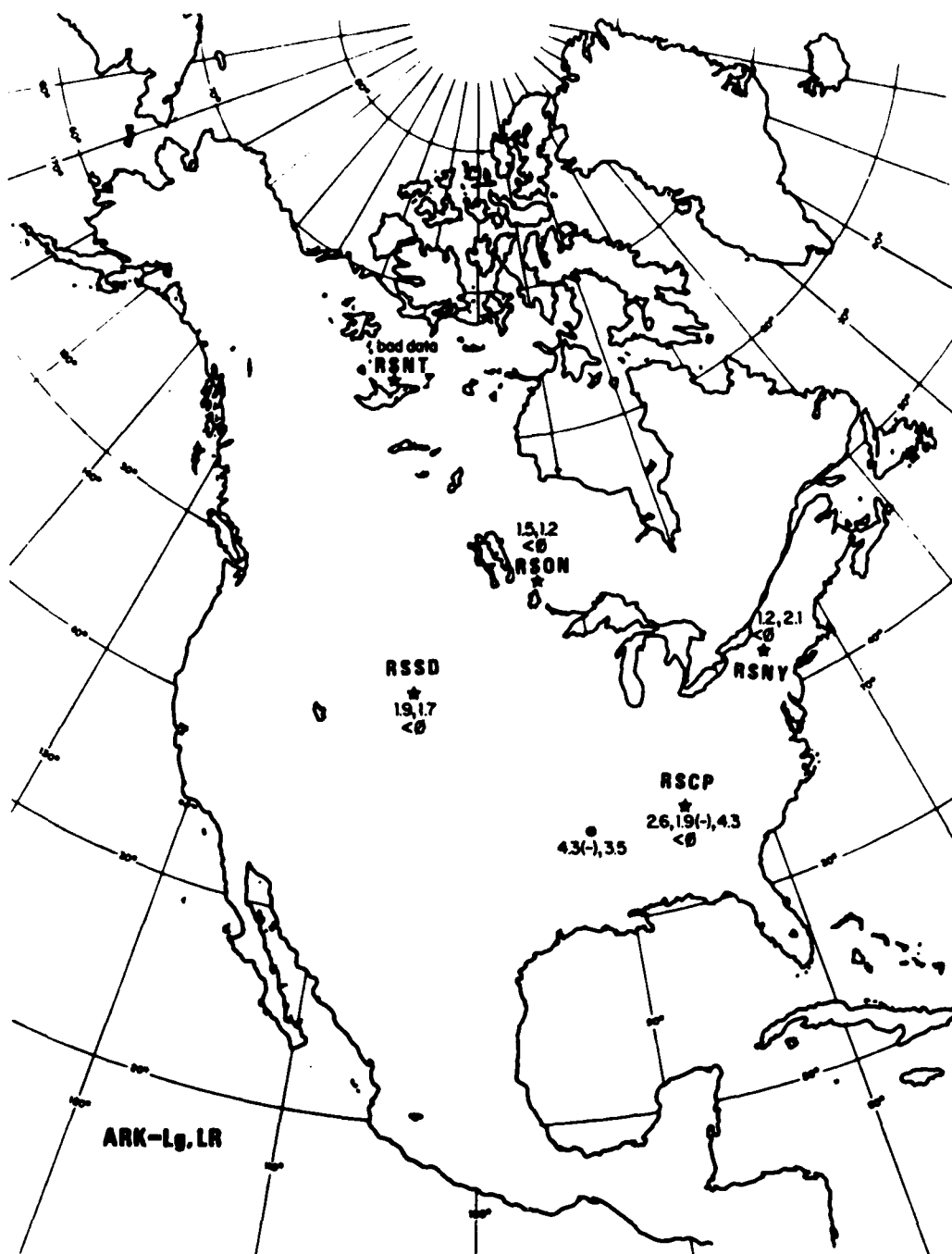
Figure 17 Arkansas earthquake Lg and L_R logarithmic signal-to-noise ratios.
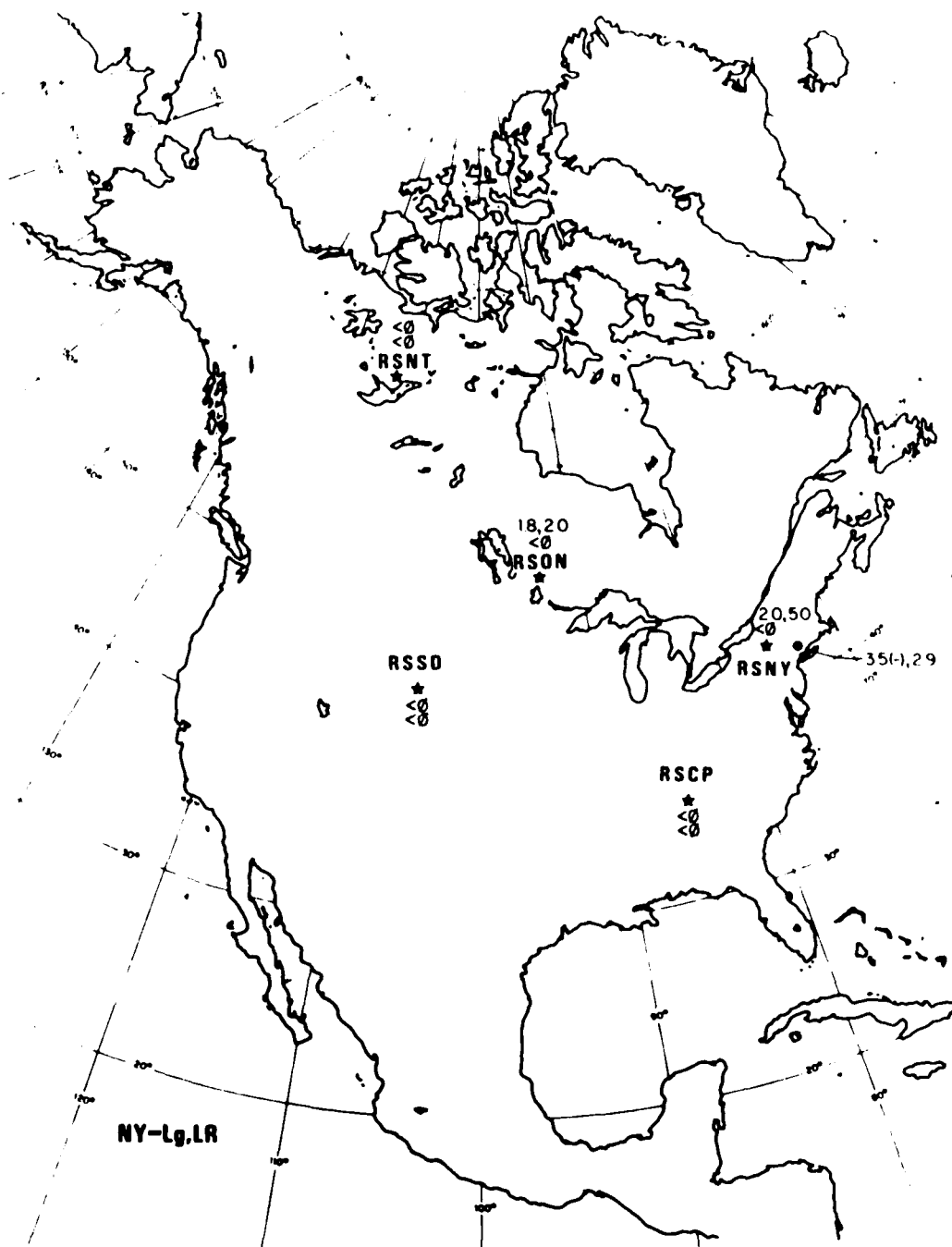
Figure 18   New York earthquake Lg and L_R logarithmic signal-to-noise ratios.
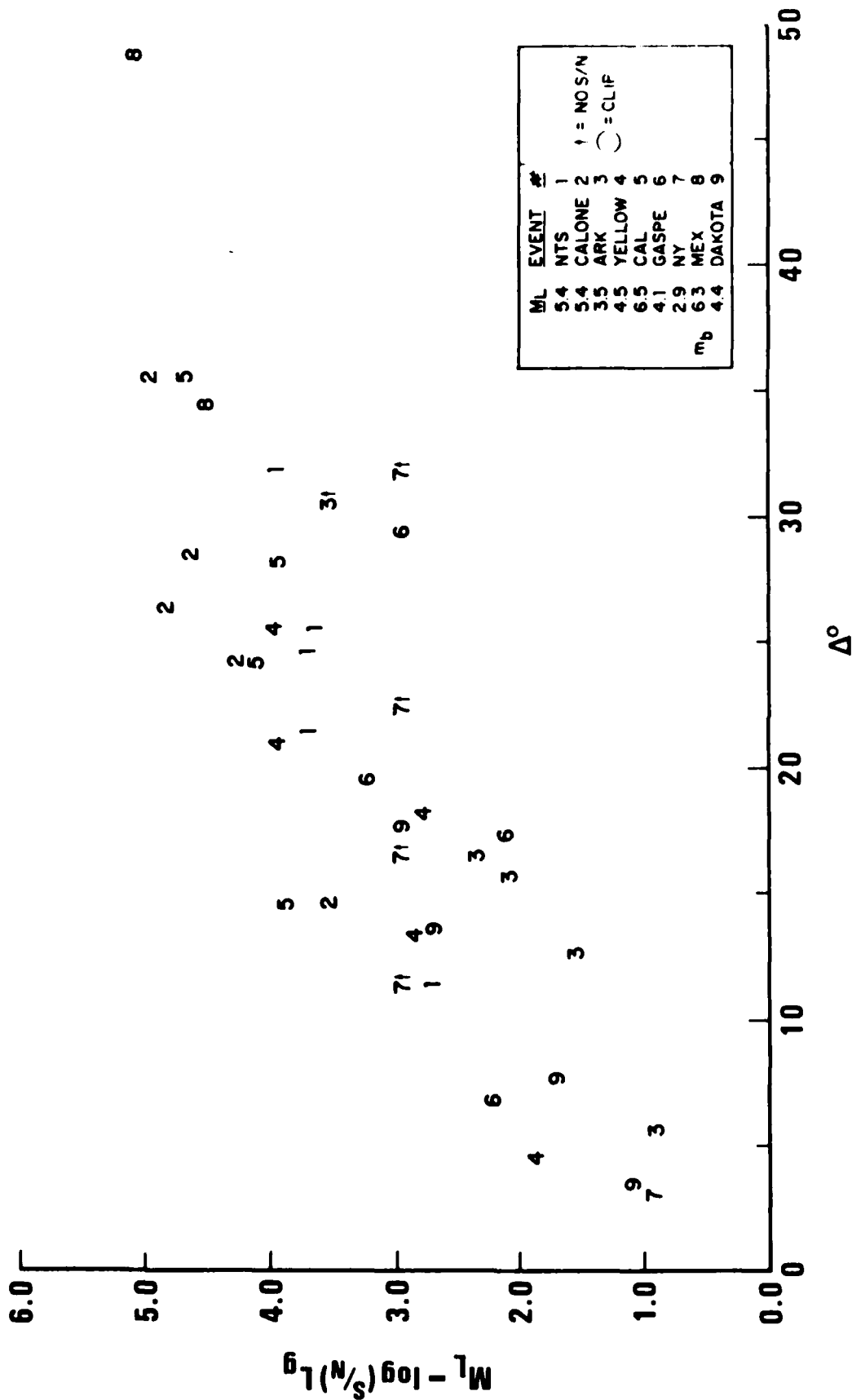
Figure 19 Lg detection threshold versus distance for the nine studied events. Lg detection thresholds are not significantly below P wave detection thresholds of Figure 14.

estimates are gathered in Figure 19 as a function of distance. The estimated L_g detection thresholds are significantly better than the estimated P-wave detection thresholds of Figure 14 for distances greater than 15 degrees. This may be an artifact that events from the tectonic provinces of North America dominate the longer paths sampled, and the larger magnitude events.

L_R detection thresholds derived from (S/N) estimates are compiled in Figure 20. The $r^{-1/2}$ curve is plotted for comparison. The large (m_b 6.3) Mexican earthquake may yield a biased estimate of the L_R detection threshold because of source scaling effects. Larger events, with corner frequencies below 1 Hz, are not adequately characterized by the 1 Hz m_b estimate. Since the m_b estimate for such an event is probably an under estimate of the low frequency L_R generated by the event, the L_R thresholds for (8), the Mexican earthquake, are biased low.
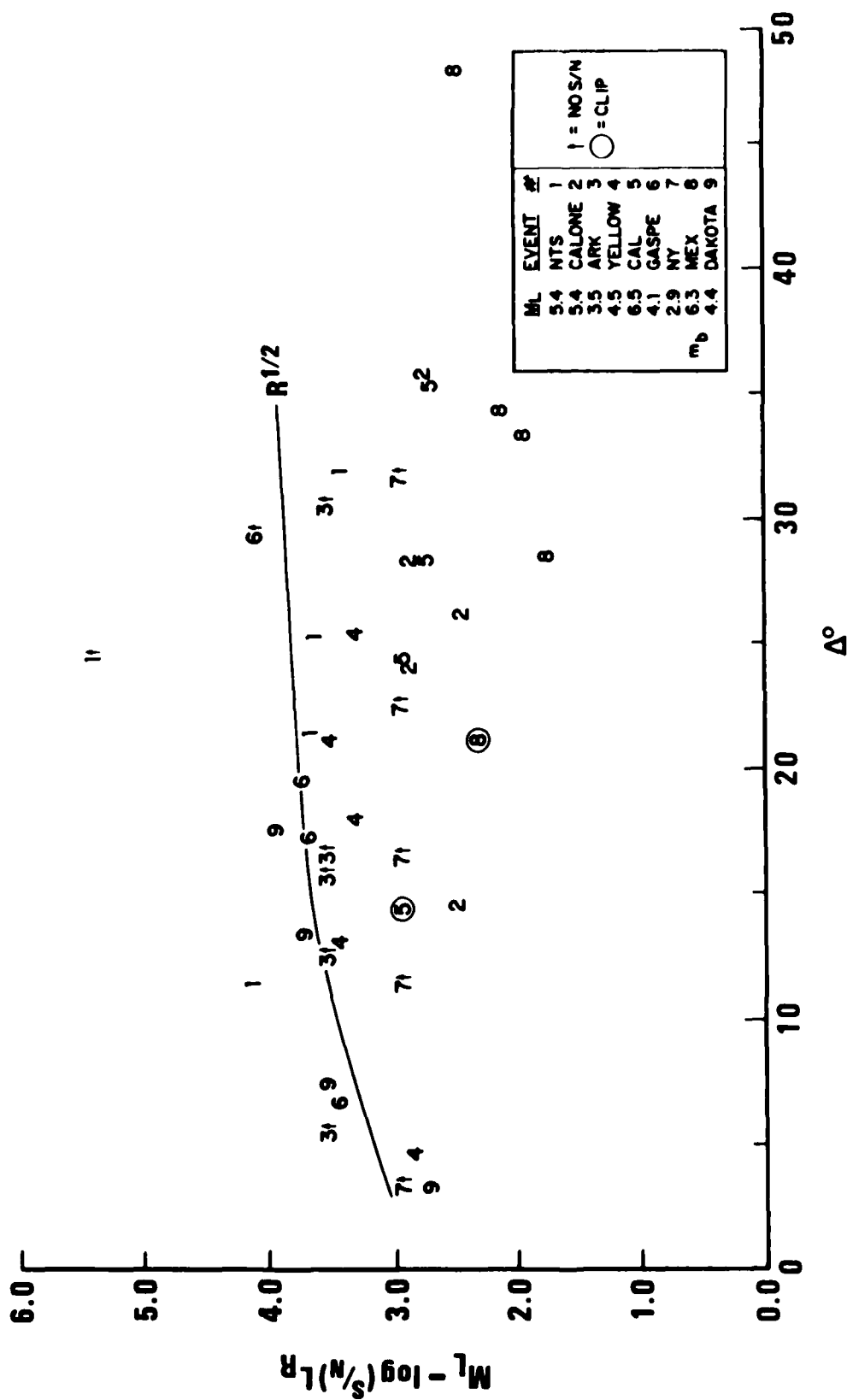
Figure 20 L_R detection thresholds versus distance derived from signal-to-noise ratios. 0's indicate clipping of signal and consequently biased estimates of detection threshold.

-34-

Data Flow at the CSS

Tapes of the RSTN data in SCARS format were directly recorded at the CSS or were obtained from SCARS by request. It was found that existing software at the CSS did not properly identify and process calibration sequences. Furthermore, dead spots were found in the digital data recorded at the CSS. These data drop-outs were usually brief intervals of zeros (c.f. Figures 21a and 21b). To alleviate the problem of drop-outs and calibration sequences, some tapes were requested from SCARS to supplement the locally recorded data. The requested SCARS tapes had significantly fewer digital drop-outs, but the problem still persisted. The data drop-outs appear to be the result of variations in the satellite signal characteristics. A detection algorithm for these brief strings of zeros was added to the Transform program resident at the CSS.

The RSTN data was passed through two programs NSSREAD and NSSTODB to the INGRES data base management system. A shell script was developed to extract the RSTN digital data and associated calibration information to a local data base consisting of seismograms and directory information. Programs display, transform and spectrum could then be used to plot the waveforms, and calculate Fourier spectra of the digital waveforms on a Tektronix storage tube terminal. The plotting format options of spectrum were modified to accomadate the desired spectral plots. A serious "bug" in the program transform was discovered that resulted in severe aliasing of the resultant spectra. Corrections were made to the program transform and tapering options were added to the algorithm. The post detection arrival detector was found to be inadequate to the task of automatic detection. The algorithm stops with its first detection and could not be modified. Data drop-outs and noise bursts confused the algorithm, and produced too many false alarms. The algorithm could not adjust its detection criteria to a changing noise environment. Amplitudes and predominant periods of the seismic phases were measured with the disp program on the Seismic Analysis Station (SAS).
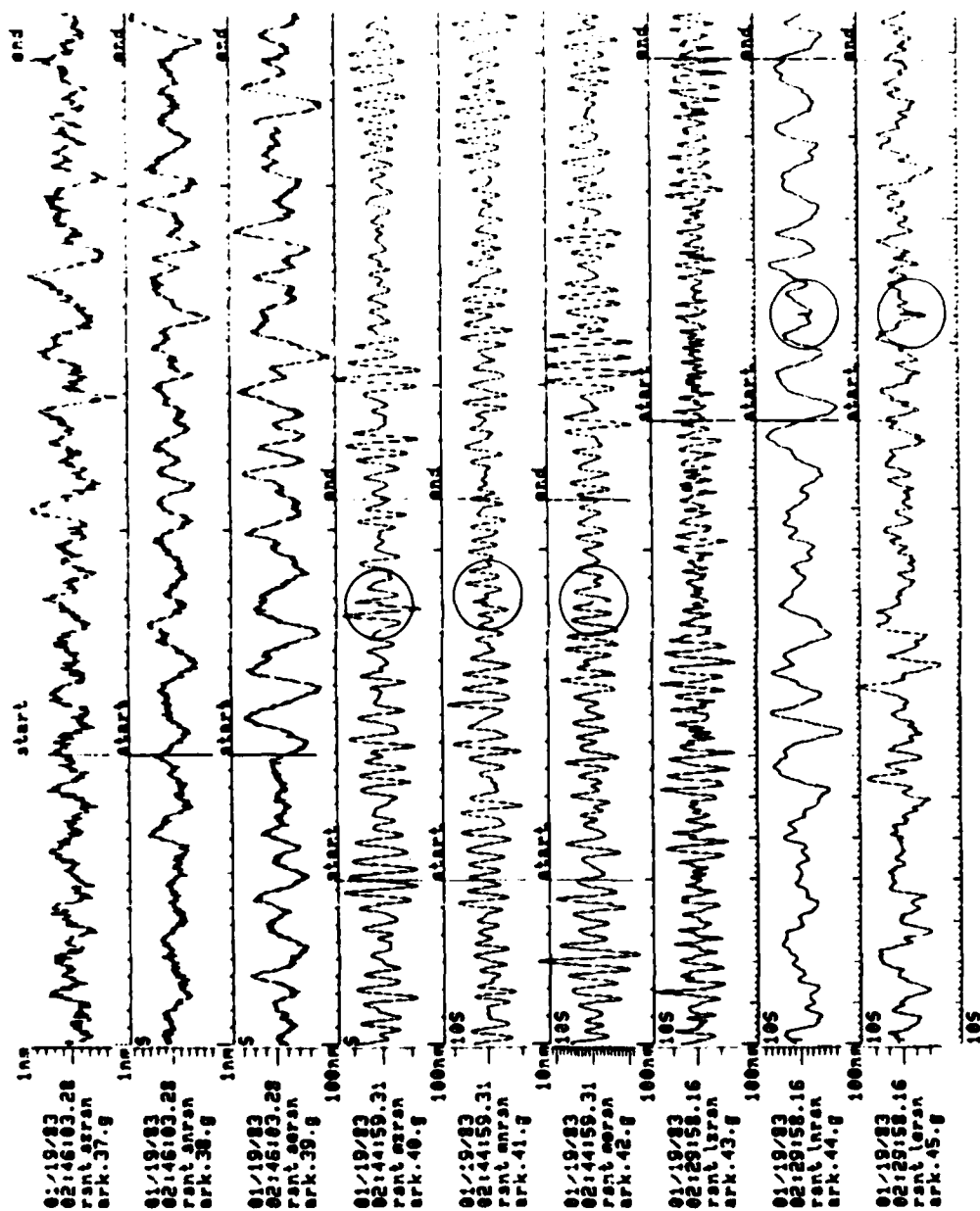
Figure 21A Example of data dropouts in middle and long perod data.
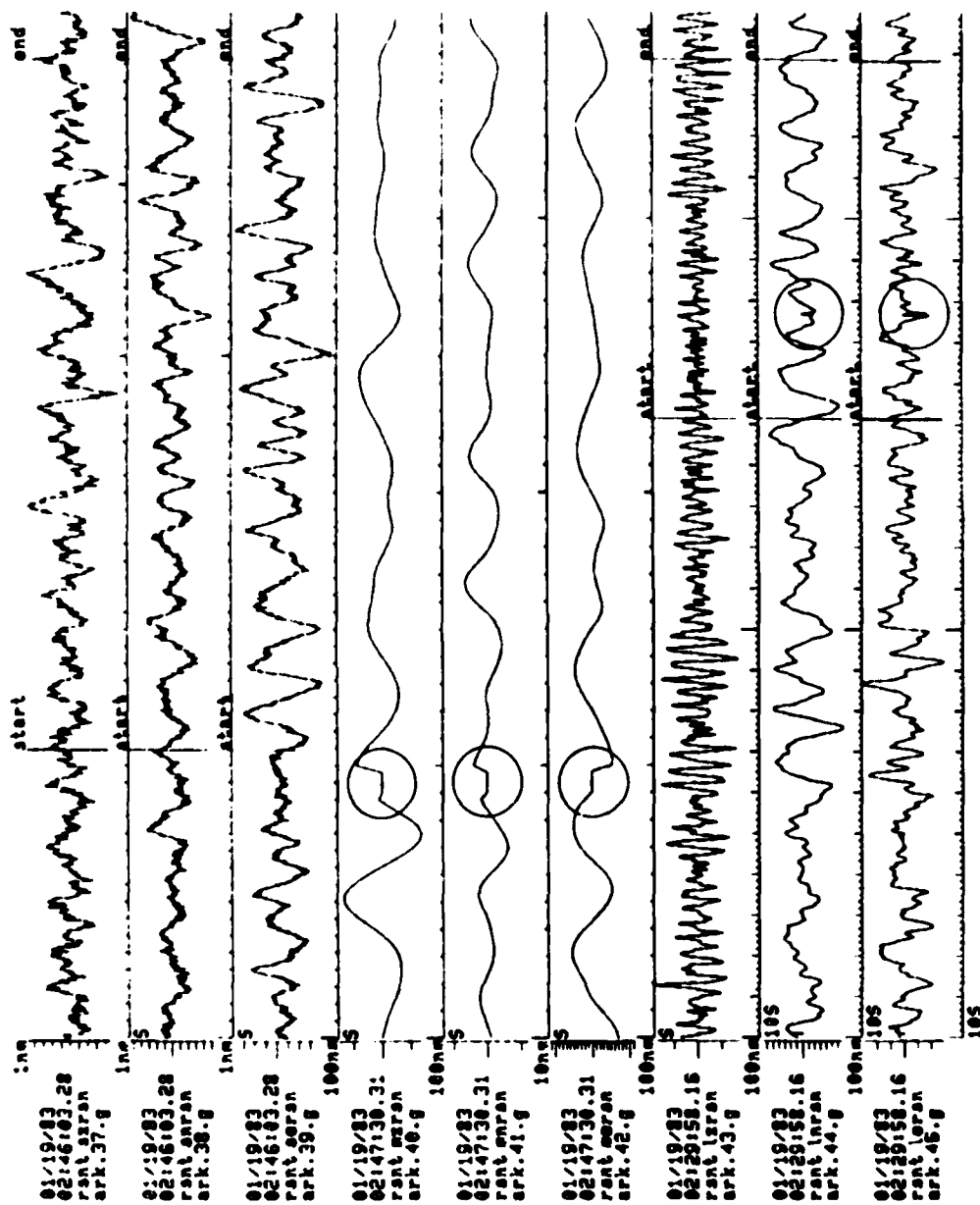
Figure 21B Expanded view of dropout of the middle period.
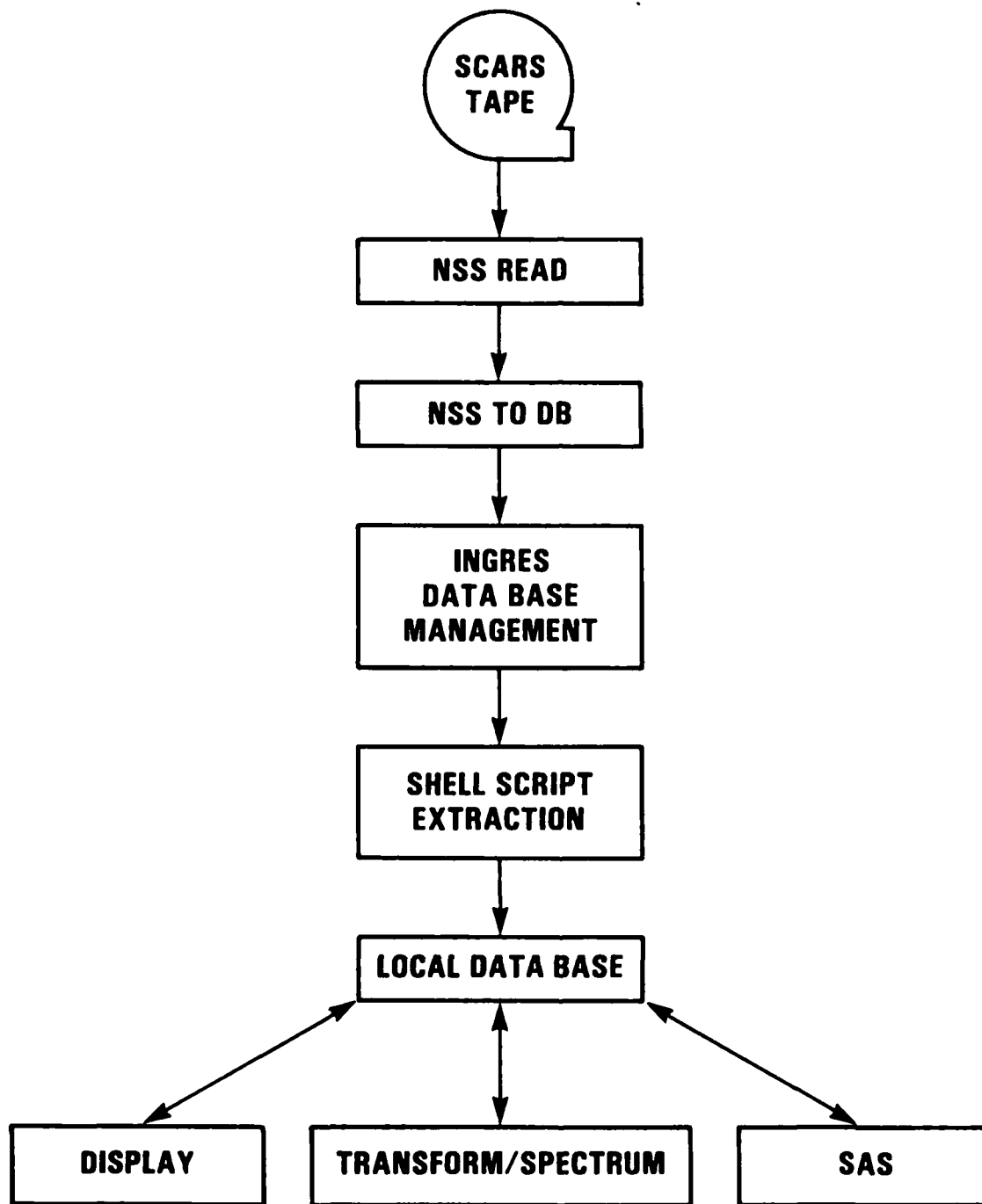
Figure 22   Data Flow at the CSS

FURTHER IMPROVEMENTS TO AUTOMATIC ASSOCIATION (AA)

Using the artificial data we had created for the International Data
Exchange Exercise, we tested Automatic Association (AA) with the
objectives of comparing its performance to Center for Seismic Studies
(CSS) AA, and to develop and include some AA features used by the
Swedish AA and the CSS AA not yet present in the Seismic Research
Center's (SRC) AA. In addition, we developed and implemented the
following features into SRC's AA.

- Kinematic/dynamic use of amplitude data

- two array event location

- use of pP and sP to attempt to automatically constrain depth

- slowness check on all phases (not just P and PKP)

- show unassociated arrivals in final summary bulletin

- include confidence ellipses in summary bulletin

A comparison of the two AA's from SRC and CSS has not been
accomplished yet, mainly because the two AA programs were executing on
different computers and a common mutually-readable data set has not been
defined.

Documentation for AA was completed and printed in Seismic Research
Information System (SRIS), (1982).

Kinematic/Dynamic Use of Amplitude

Theoretical basis for this work has been described in a memorandum by R. R. Blandford dated 7 October 1982 and a practical embodiment of the scheme is described in another memorandum by Blandford dated 19 April 1983. (Both memoranda are contained in Appendix II). An efficient Newton-Raphson procedure for computing the maximum likelihood magnitude (Ringdal, 1976) offers a computational improvement.

For a chosen network of stations, not necessarily the full network of detecting station, a maximum likelihood estimate of body wave magnitude m_b using the amplitudes of the locating arrivals. Clearly there are three special cases to consider regarding the network of "reliable" stations, the stations that actually detected, and the amplitudes of the detections.

1) A station does not report a detection even though the m_b indicates that it should have detected. 2) A station reports a detection and the m_b indicates that it should not have detected. 3) A station reports a detection but the amplitude is either too high or too low according to the m_b. Figure 23 shows the the numerical modification to the accumlated screen points for these three cases, and Figure 24 is an up to date list of the numerical values for the attributes considered in the SCREEN subroutine.

-40-

- SELECT "RELIABLE STATIONS", GET DETECTION THRESHOLDS

- COMPUTE RINGDAL M_B

- IF A STATION DID NOT DETECT BUT SHOULD HAVE,
  SUBTRACT POINTS, i.e.:

  IF $P(DET) > .95$: -1.0

      $P(DET) > .99$: -2.0

- IF A STATION DID DETECT AND REPORTS AN 'UNUSUAL'
  AMPLITUDE, A_0, DISCARD THAT AMPLITUDE FOR THIS EVENT,

  IF $P(AMP > A_0) < .01$ OR

      $P(AMP < A_0) < .01$ THEN REJECT A_0, START SCREEN OVER

- IF A STATION DID DETECT BUT SHOULD NOT HAVE, DISCARD
  ALL POINTS DUE TO THAT STATION, i.e.:

  IF $P(DET) < .01$, $-$ (ALL POINTS DUE TO STATION)

Figure 23 Amplitude Modifications to SCREEN

-41-

AUTOMATIC DETECTION: + 0.82

    IF (θ) AND $\Delta < 90^{\circ}$:   + 1.02

    IF (R) AND $\Delta < 7^{\circ}$:   + 0.85

ANALYST - CERTIFIED DETECTIONS: + 0.98

    IF (θ) AND $\Delta < 90^{\circ}$:   + 1.18

    IF (p) AND $\Lambda < 90^{\circ}$:   + 0.89

    IF (R) AND $\Lambda < 7^{\circ}$:   + 1.10

IF IN SHADOW ZONE: - 0.65

IF S PHASE: + 1.10

IF IN CODA: - 0.20

IF SLOWNESS ERROR LARGE: - 1.07

IF NO LATER PHASES   - 0.50

5 POINTS REQUIRED FOR DECLARATION

10 POINTS IN A-SEISMIC ZONE

Figure 24 SCREEN Points

Depth Constraint with pP and sP

Our experience with analyst-named phases indicates a tendency to
name the teleseismic phase next arriving after P as pP. In fact, the
next arriving phase may not be pP, but it may be sP, PcP or some
unidentified phase. Restraining depth to the analyst's P-pP time during
location convergence could lead to difficulties in correct event
location and association of phases.

These considerations lead to the "soft" treatment of pP and sP named
phases described here.

The list of P arrivals that is about to be input to the HYPO
location program is examined in time order. The arrival queue is
searched for a detection at the same station that is labeled pP or sP.
If an sP is found the search terminates and the depth for P-sP is used
as an input depth to HYPO. HYPO is not constrained to this depth,
however. If no sP is found, the smallest P-pP time, if any are found,
is used to establish the input depth to HYPO, again unrestrained to
depth. The idea here is to try to improve the initial depth estimate of
the HYPO solution.

The situation where the depth is actually constained by labeled pP
or sP phases occurs as follows. When an event has been made and fully
associated, its detections are examined to see if there is an sP phase,
labeled as such by AA, which had also been labeled sP by the analyst.
If one is found this P-sP depth is used to constrain HYPO and the event
is run again. If no sP is found, the same algorithm is applied to P-pP
depth, using the smallest P-pP time, if any. This algorithm works very
well with the artificial data because analyst labeled "sP" is always
true in this data set. More work has to be done on this algorithm to
expand its usefulness to real data.

Other AA Improvements

In addition to the two major improvements described above some
continuing enhancements to AA were accomplished. The slowness check has
been extended to include all phases recognized by AA. Previously the
slowness check was limited to P and PKP phases during the location
phase. Since the travel times for the remaining phases are computed by
polynomial evaluation rather than by table lookup, this necessitated the
creation of a complete, new program component in which there is
duplication of several of the computational modules used in travel time
determinations during location.

Two array station trial epicenters have been added, based on the
intersection of their respective confidence ellipses. SRC's AA uses
this as the last pass through the signal queue, so in general, very few
events are started this way. It has been added to be compatible with
other AA programs. Equations for the two array computation are shown in
Figure 25.

Confidence ellipse information has been added to the summary
bulletin in accordance with standard practice.

The format of the summary bulletin has been expanded so that
"left-over" or unassociated detections are printed in-line with the
events and their association. This printing is a great help in
reviewing the bulletin and the performance of AA. Various printing
highlights are used to make the unassociated detections differentiate
from the associated detections.

$$
\text{ARRAY 1} \begin{cases} \delta P_X^1 = \dfrac{\partial P_X^1}{\partial \theta}\, d\theta + \dfrac{\partial P_X^1}{\partial \psi}\, d\psi + \dfrac{\partial P_X^1}{\partial h}\, dh \\[2em] \delta P_Y^1 = \dfrac{\partial P_Y^1}{\partial \theta}\, \delta\theta + \,.. \\[2em] \delta T^1 = \dfrac{\partial T^1}{\partial \theta}\, \delta\theta + \,... \qquad\qquad + \delta T_0 \end{cases}
$$

$$
\text{ARRAY 2} \begin{cases} \delta P_X^2 = \dfrac{\partial P_X^2}{\partial \theta}\, \delta\theta + \,.. \\[2em] \delta P_Y^2 = \dfrac{\partial P_Y^2}{\partial \theta}\, \delta\theta + \,... \\[2em] \delta T^2 = \dfrac{\partial T^2}{\partial \theta}\, \delta\theta + \,... \qquad\qquad + \delta T_0 \end{cases}
$$

OR

$$
\underline{\delta} = B \underline{dx}
$$

$$
\underline{dx} = (B^T \Sigma^{-1}\ B)^{-1}\ B^T \Sigma^{-1}\ \underline{\delta}
$$

Σ CONTAINS TRAVEL TIME AND SLOWNESS ERROR VARIANCE ESTIMATES
DOWN THE DIAGONAL

Figure 25   Two-Array Location

Future Improvements

As mentioned earlier, further work needs to be done using pP as a depth constraint with real data. Methods have to be worked out for making best use of the depth phase information in the signal arrival queue, and probably for making a choice of different algorithms. In some cases no uses at all would be made of pP and sP, and automatic methods to determine that this would be the best strategy needed.

We believe that the capabilities of AA ought to be expanded to include and make use of regional phases. There are six local phases: Pn, Pg, P, Sn, Sg and S. The program ACLOC uses regional phases as well as array information and other later phases for location. ACLOC would replace HYPO in AA. Conceptually, this is fairly straight-forward, but considerable programming effort is required to make the resulting large package manageable.

REFERENCES

Breding, D. R. (1982). Data User's Guide for the Regional Seismic Test
    Network (RSTN). Sandia National Laboratories, Albequerque, N. M.,
    SAND-82-2935.

Bungum, H. (1983), L. B. Tronrud (ed) (1983). NORSAR Scientific Report
    No. 2-82/83 Semianual Technical Summary (June 1983).

Fix, J. E. (1972). Ambient Earth Motion in the Period Range from 0.1 to
    2560 Sec BSSA 62 No 6 pp 1753-1760.

Herrin, E. (1982). The resolution of Seismic Instruments Used in Treaty
    Verification Research. BSSA 72 #6 pp S61-S67.

Openheim, A. V. and R. W. Schafer (1975). Digital Signal Processing,
    Prentice - Hall 585 pages

Owens, T. J., S. R. Taylor and G. Zandt (1983). Crustal Structure
    beneath RSTN stations Inferred from Teleseismic P-waveforms.
    Preliminary results at RSCP, RSSD, and RSNY, VCID-19859

Ringdal, F. (1976). Maximum likelihood estimation of seismice
    magnitude, Bull. Seism. Soc. Am. 66, 789-802.

Rodgers, P. W. and M. Hummel (1981). National Seismic Stations
    transducers and filters, Lawrence L. N. L., Livermore, Ca.
    VCRL-53093

Seismic Research Information System (SRIS), Program Specification for
    Automatic Association (1982). Geotech Alexandria Laboratory,
    Alexandria, Va.

Taylor, S. R. and B. J. Qualheim (1983). Regional Seismic Test Network
    Site Descriptions, Lawrence Livermore Laboratory Report -
    VCID-19769

(THIS PAGE INTENTIONALLY LEFT BLANK)

APPENDIX I

AMPLITUDES AND PERIODS AT RSTN STATIONS

ARK BSCP Delta = 5.44, Azimuth = 287.50, 63/019/0850:40.5														
	SP					MP					LP			
Phase	Amp	T(sec)	(S/N)	F(Hz)	Phase	Amp	T(sec)	(S/N)	F(Hz)	Phase	Amp	T(sec)	(S/N)	F(Hz)
Pz	42	0.325	29	4.0	Pz	20	2.5	157	1.63	-	-	-	-	-
Pn	14	0.25	15	3.4	Pn	9	3.5	100	1.62	-	-	-	-	-
Pe	24	0.325	20	2.5	Pe	17	3.0	20	1.63	-	-	-	-	-
Lgz	864	0.275	333	1.9	Lgz	91	0.75	143	1.57	-	-	-	-	-
Lgn	576	0.35	250	2.6	Lgn	95	1.0	95	1.71	-	-	-	-	-
Lge	581	0.225	364	4.3	Lge	36	0.5	285	1.57	-	-	-	-	-

ARK BSNT Delta = 30.71, Azimuth = 148.37, 63/019/0850:40.5														
	SP					MP					LP			
Phase	Amp	T(sec)	(S/N)	F(Hz)	Phase	Amp	T(sec)	(S/N)	F(Hz)	Phase	Amp	T(sec)	(S/N)	F(Hz)
Lgz	3.8	1.47	-	-	-	-	-	-	-	-	-	-	-	-
Lgn	2.0	1.575	-	-	-	-	-	-	-	-	-	-	-	-
Lge	2.5	1.375	-	-	-	-	-	-	-	-	-	-	-	-

ARK BSNY Delta = 16.46, Azimuth = 361.44, 63/019/0222:43.5														
	SP					MP					LP			
Phase	Amp	T(sec)	(S/N)	F(Hz)	Phase	Amp	T(sec)	(S/N)	F(Hz)	Phase	Amp	T(sec)	(S/N)	F(Hz)
Pz	2.2	0.2	3	2.25	-	-	-	-	-	-	-	-	-	-
Pz	2.2	0.2	3	3.65	-	-	-	-	-	-	-	-	-	-
Pn	2.9	0.325	4	3.0	-	-	-	-	-	-	-	-	-	-
Pe	1.75	0.225	-	-	-	-	-	-	-	-	-	-	-	-
Lgz	9.6	0.65	15	2.1	Lgz	16	1.25	4	1.32	-	-	-	-	-
Lgn	13	0.675	13	2.6	Lgn	11	1.5	5	1.37	-	-	-	-	-
Lge	11	0.775	5	2.0	Lge	22	2.0	5	1.26	-	-	-	-	-

ARK BSON Delta = 15.71, Azimuth = 175.51, 63/019/0222:43.5														
	SP					MP					LP			
Phase	Amp	T(sec)	(S/N)	F(Hz)	Phase	Amp	T(sec)	(S/N)	F(Hz)	Phase	Amp	T(sec)	(S/N)	F(Hz)
Pz	3.0	0.25	10	2.7	-	-	-	-	-	-	-	-	-	-
Pz	3.0	0.25	5	6.0	-	-	-	-	-	-	-	-	-	-
Pn	1.4	0.35	6	4.1	-	-	-	-	-	-	-	-	-	-
Pe	1.0	0.225	3	6.0	-	-	-	-	-	-	-	-	-	-
Lgz	7	0.625	6	1.65	Lgz	27	1.75	15	1.29	-	-	-	-	-
Lgn	5	0.925	30	1.15	Lgn	31	2.0	10	1.23	-	-	-	-	-
Lge	29	1.1	30	1.65	Lge	56	1.75	30	.87	-	-	-	-	-

ARK BSSD Delta = 12.74, Azimuth = 133.48, 63/019/0230:43.5														
	SP					MP					LP			
Phase	Amp	T(sec)	(S/N)	F(Hz)	Phase	Amp	T(sec)	(S/N)	F(Hz)	Phase	Amp	T(sec)	(S/N)	F(Hz)
Pz	8.4	0.4	4	15	-	-	-	-	-	-	-	-	-	-
Pz	8.4	0.4	5	3.6	-	-	-	-	-	-	-	-	-	-
Pn	4.4	0.35	-	-	-	-	-	-	-	-	-	-	-	-
Pe	3.6	0.4	-	-	-	-	-	-	-	-	-	-	-	-
Lgz	18	0.575	40	1.5	Lgz	31	1.75	31	1.2	-	-	-	-	-
Lgn	35	0.675	17	1.25	Lgn	20	1.5	50	1.13	-	-	-	-	-
Lge	32	0.675	63	1.7	Lgn	35	1.2	45	1.265	-	-	-	-	-

CAL ESCP Delta = 28.03, Azimuth = 281.604, 03/18?/23:42:37.9

Phase	Amp	T(sec)	(S/N)	F(Hz)	Phase	Amp	T(sec)	(S/N)	F(Hz)	Phase	Amp	T(sec)	(S/N)	F(Hz)
		SP					MP					LP		
Pz	363.3	0.6	17	1.35	Pz	580.4	2.25	800	.05	Pz	8827.7	21	10	.045
Pn	44.9	0.625	30	1.7	Pn	48.4	1.75	96	.09	Pn	1890.4	22	36	.04
-	-	-	-	-	-	-	-	-	-	Pn	1890.4	22	30	.17
Pe	128.3	0.75	140	1.7	Pe	262.1	1.75	300	.05	Pe	4374.6	21	200	.041
-	-	-	-	-	-	-	-	-	-	Pe	4374.6	21	40	.16
Lgz	478.1	2.625	57	.3	Lgz	8724.4	7.0	8000	.055	-	-	-	-	-
-	-	-	-	-	Lgz	8724.4	7.0	1288	.166	-	-	-	-	-
Lgn	440.6	2.85	350	.3	Lgn	14492.1	6.25	10000	.055	-	-	-	-	-
Lge	280.2	2.675	150	.3	Lge	5704.9	6.5	5000	.055	-	-	-	-	-
-	-	-	-	-	Lrz	30218.1	8.75	6000	.11	Lrz	86891.9	19	8400	.16
-	-	-	-	-	Lrn	9181.7	8.75	3333	.1	Lrn	185925	21	6000	.091
-	-	-	-	-	Lre	26363.2	8.75	10000	.1	Lre	60129.9	19	4000	.15

CAL ESNY Delta = 35.4, Azimuth = 578.6, 03/18?/23:42:37.9

Phase	Amp	T(sec)	(S/N)	F(Hz)	Phase	Amp	T(sec)	(S/N)	F(Hz)	Phase	Amp	T(sec)	(S/N)	F(Hz)
		SP					MP					LP		
Pz	33.7	1.05	20	1.2	Pz	370.1	3.85	143	.035	Pz	3436.9	19.0	167	.1
Pn	6.87	0.6	3.75	1.3	Pn	36.1	3.85	14	.07	Pn	563.2	19.0	60	.035
Pe	21.1	1.0	11	1.0	Pe	227.2	2.75	154	.035	Pe	2891.8	20.0	266	.035
-	-	-	-	-	-	-	-	-	-	Pe	2891.8	20.0	63	.12
Lgz	114.5	2.975	56	.3	Lgz	4004.8	6.85	2333	.05	-	-	-	-	-
Lgn	234.2	3.2	67	.3	Lgn	9226.1	7.75	3846	.05	-	-	-	-	-
Lge	87.0	3.425	20	.3	Lge	1591.3	7.0	2000	.03	-	-	-	-	-
-	-	-	-	-	Lrz	279420	10.0	4615	1.1	Lrz	113920.015.0	7000	.1	
-	-	-	-	-	Lrn	13676	11.85	8857	.05	Lrn	165297	20.0	5000	.045
-	-	-	-	-	Lre	20353.8	8.85	7500	1.1	Lre	79056.5	15.0	6667	.033
-	-	-	-	-	-	-	-	-	-	Lre	79056.5	15.0	4714	.11

CAL ESOR Delta = 24.07, Azimuth = 362.70, 03/18?/23:42:37.9

Phase	Amp	T(sec)	(S/N)	F(Hz)	Phase	Amp	T(sec)	(S/N)	F(Hz)	Phase	Amp	T(sec)	(S/N)	F(Hz)
		SP					MP					LP		
Pz	205.3	0.575	400	1.2	Pz	2114.9	3.75	667	.04	Pz	12365.5	21	1000	.03
-	-	-	-	-	Pz	2114.9	3.75	40	1.0	-	-	-	-	-
Pn	34.7	0.6	100	1.6	Pn	616.9	3.0	228	.04	Pn	4914.3	24	266	.04
-	-	-	-	-	Pn	616.9	3.0	14	.08	-	-	-	-	-
Pe	163.9	0.675	500	1.5	Pe	1375.4	3.85	1200	.04	Pe	10021.7	23	1000	.04
-	-	-	-	-	Pe	1375.4	3.85	85	1.0	-	-	-	-	-
Lgz	198.1	2.725	250	.3	Lgz	5052.0	6.0	8867	.03	-	-	-	-	-
-	-	-	-	-	Lgz	5052.0	6.0	138	.89	-	-	-	-	-
Lgn	114.2	2.925	222	.3	Lgn	6997.9	5.0	3333	.045	-	-	-	-	-
-	-	-	-	-	Lgn	6997.9	5.0	400	.21	-	-	-	-	-
Lge	130.0	3.2	222	.3	Lge	2529.2	4.75	8000	.065	-	-	-	-	-
-	-	-	-	-	Lge	25292.2	4.75	300	.25	-	-	-	-	-
-	-	-	-	-	Lrz	30210.1	10.5	8871	.1	Lrz	180156.0	13	4986	.035
-	-	-	-	-	Lrn	22760.9	10.0	8979	.1	Lrn	107055.0	18	4187	.035
-	-	-	-	-	Lre	21145.1	10.0	80000	.075	Lre	111307	19	4000	.04

CAL. REED Delta = 14.68, Azimuth = 363.16, 08/188/18:48:37.9														
	SP					MP					LP			
Phase	Amp	T(sec)	(S/N)	F(Hz)	Phase	Amp	T(sec)	(S/N)	F(Hz)	Phase	Amp	T(sec)	(S/N)	F(Hz)
Pz	94.4	1.275	62.5	.75	Pz	1485.2	4.25	800	.08	Pz	83687.7	18	7143	.036
Pz	-	-	-	-	Pz	1485.2	4.25	00	1.2	Pz	83687.7	18	350	.12
Pn	58.0	1.25	30	.75	Pn	842.6	3.75	850	.08	Pn	106016	18	500	.053
-	-	-	-	-	Pn	842.6	3.75	40	1.3	Pn	106016	18	350	.1
Pe	86.6	1.025	14	.75	Pe	1475.6	3.5	1333	0.7	Pe	83673.0	18	1333	.03
-	-	-	-	-	Pn	1475.6	3.5	185	.06	Pe	83673.0	18	3000	.01
Lgz	488.3	1.56	454	.3	Lgz	12573.6	5.25	8800	.03	-	-	-	-	-
-	-	-	-	-	Lgz	12573.6	5.25	454	.07	-	-	-	-	-
Lgn	465.0	1.475	800	.8	Lgn	6888.2	5.0	4865	.035	-	-	-	-	-
Lge	380.6	1.56	850	1.1	Lge	6885.12	5.0	8800	.045	-	-	-	-	-
-	-	-	-	-	Lrz	30816	8.75	5000	.1	Lrz	105687	33	5555	.043
-	-	-	-	-	-	-	-	-	-	Lrz	105687	33	5000	.16
-	-	-	-	-	Lrn	30816	10	10000	.1	Lrn	107388	18	5666	.031
-	-	-	-	-	-	-	-	-	-	Lrn	107388	18	10555	.010
-	-	-	-	-	Lre	30816	8.50	14888	.1	Lre	141083	17	13333	.032
-	-	-	-	-	-	-	-	-	-	Lre	141083	17	88571	.082

GASPE NSCP Delta = 19.80, Azimuth = 39.81, 83/017/1835:51.0

	SP					MP					LP			
Phase	Amp	T(sec)	(S/N)	F(Hz)	Phase	Amp	T(sec)	(S/N)	F(Hz)	Phase	Amp	T(sec)	(S/N)	F(Hz)
Pz	14.6	0.325	-	-	Pz	-	-							
Pn	6.7	0.325	-	-	Pn	-	-							
Pe	11.4	0.325	-	-	Pe	-	-	-	-					
Lgz	49.4	0.7	8	1.3	Lgz	41.9	1.5	6	1 2	-	-	-	-	-
Lgn	34.4	0.65	8	1.3	Lgn	35.0	1 5	6	1 1	-	-	-	-	-
Lge	33.5	0.625	6	1.3	Lge	26.0	1.75	6	1.275	-	-	-	-	-
-	-	-	-	-	-	-	-	-	-	Lrz	76.9	19.0	-	-
-	-	-	-	-	-	-	-	-	-	Lrn	59.9	23.0	2.5	.037
-	-	-	-	-	-	-	-	-	-	Lre	46.2	20.0	-	-

GASPE RSNT Delta = 89.16, Azimuth = 94.67, 83/017/1835:51.0

	SP					MP					LP			
Phase	Amp	T(sec)	(S/N)	F(Hz)	Phase	Amp	T(sec)	(S/N)	F(Hz)	Phase	Amp	T(sec)	(S/N)	F(Hz)
Pz	1.3	0.6	?	?	-	-	-	-	-	-	-	-	-	-
Pn	-	-	2	2.3	-	-	-	-	-	-	-	-	-	-
Pe	1.1	0.65	4	2.7	-	-	-	-	-	-	-	-	-	-
Lgz	14.3	1.475	6	1	Lgz	17.3	1.5	20	1.07	-	-	-	-	-
Lgn	21.8	1.0	2	2	Lgn	34.6	1.5	50	1.12	-	-	-	-	-
Lge	11.4	1.15	16	1.7	Lge	8.0	1.5	31	1.1	-	-	-	-	-

GASPE RSNY Delta = 6.9, Azimuth = 45.94, 83/017/1835:51.0

	SP					MP					LP			
Phase	Amp	T(sec)	(S/N)	F(Hz)	Phase	Amp	T(sec)	(S/N)	F(Hz)	Phase	Amp	T(sec)	(S/N)	F(Hz)
Pz	21.9	0.25	84	4.2	Pz	-	-	-	4.4	1.07	-	-	-	-
Pz	21.9	0.25	35	7.1	-	-	-	-	-	-	-	-	-	-
Pn	17.2	0.35	25	4.1	Pn	-	-	5	1.1	-	-	-	-	-
Pe	15.6	0.325	33	4.3	Pe	-	-	4.2	1.1	-	-	-	-	-
Pe	15.6	0.325	25	6.4	-	-	-	-	-	-	-	-	-	-
Lgz	207.8	0.475	60	2.1	Lgz	146.1	1.5	26.7	1.17	-	-	-	-	-
Lgn	175.0	0.55	60	1.65	Lgn	154.0	1.0	36	1.27	-	-	-	-	-
Lgn	175.0	0.55	50	6.3	-	-	-	-	-	-	-	-	-	-
Lge	212.0	0.75	75	1.6	Lge	283	1.0	70	1.18	-	-	-	-	-
Lge	212.0	0.75	50	5.8	-	-	-	-	-	-	-	-	-	-
-	-	-	-	-	-	-	-	-	-	Lrz	141.5	11.0	4.3	.051
-	-	-	-	-	-	-	-	-	-	Lrn	1110	12.0	2.2	.047
-	-	-	-	-	-	-	-	-	-	Lre	110.0	9.0	5.0	.04

GASPE RSON Delta = 17.94, Azimuth = 95.41, 83/017/1835:51.0

	SP					MP					LP			
Phase	Amp	T(sec)	(S/N)	F(Hz)	Phase	Amp	T(sec)	(S/N)	F(Hz)	Phase	Amp	T(sec)	(S/N)	F(Hz)
Pz	2.3	0.35	6.7	4.4	Pz	-	-	-	-	-	-	-	-	-
Pn	1.3	0.3	10	4.3	Pn	-	-	-	-	-	-	-	-	-
Pe	0.9	0.35	10	4.3	Pe	-	-	-	-	-	-	-	-	-
Lgz	62.2	0.625	67	1.6	Lgz	36.6	1.25	22	1.17	-	-	-	-	-
-	-	-	-	-	Lgz	36.6	1.25	40	1.45	-	-	-	-	-
Lgn	46.6	0.7	100	1.5	Lgn	53.4	1.0	40	1.15	-	-	-	-	-
Lge	46.9	0.785	52	1.55	Lge	33.1	1.5	16	1.06	-	-	-	-	-
-	-	-	-	-	Lge	33.1	1.5	40	1.49	-	-	-	-	-
-	-	-	-	-	-	-	-	-	-	Lrz	57.6	18.0	2.86	.055
-	-	-	-	-	-	-	-	-	-	Lrn	73.6	15.0	-	-
-	-	-	-	-	-	-	-	-	-	Lre	41.6	15.0	2.5	.056

MRK MRCP Delta = 91.3, Azimuth = 305.44, 63/094/0017:38.6

	SP					MP					LP			
Phase	Amp	T(sec)	(S/N)	F(Hz)	Phase	Amp	T(sec)	(S/N)	F(Hz)	Phase	Amp	T(sec)	(S/N)	F(Hz)
Pz	747.9	0.525	666.6	1.6	Pz	672.3	1.75	200	.07	Pz	31791.6	17.0	625	.043
-	-	-	-	-	Pz	672.3	1.75	100	.96	-	-	-	-	-
Pn	365.5	0.55	666.6	2.0	Pn	354.2	1.5	375	.06	Pn	19059.6	20.0	600	.036
-	-	-	-	-	Pn	354.2	1.5	66.6	.79	-	-	-	-	-
Pe	381.7	0.6	500.0	2.0	Pe	159.6	1.25	100	.055	Pe	10350.8	18.0	1633	.04
Lgz	-	-	114	1.6	-	-	-	-	-	-	-	-	-	-
Lgn	-	-	200	1.7	-	-	-	-	-	-	-	-	-	-
Lge	-	-	233.3	1.9	-	-	-	-	-	-	-	-	-	-
-	-	-	-	-	Lrz	4699.3	32.6	10000	.035	Lrz	165927	33	10000	.035
-	-	-	-	-	Lrn	5961.1	30.6	3333	.035	Lrn	131016.089.0		6666	.035
-	-	-	-	-	Lre	5862.3	34.6	60003	.035	Lre	165327	36.0	10000	.035

MRK MSNT Delta = 46.94, Azimuth = 164.72, 63/094/0017:38.6

	SP					MP					LP			
Phase	Amp	T(sec)	(S/N)	F(Hz)	Phase	Amp	T(sec)	(S/N)	F(Hz)	Phase	Amp	T(sec)	(S/N)	F(Hz)
Pz	91.9	0.675	333.3	2.0	Pz	1524.2	3.0	100	.04	Pz	3052.1	14.0	220	.032
-	-	-	-	-	Pz	1524.2	3.0	250	1.0	-	-	-	-	-
Pn	46.9	0.55	400	1.4	Pn	807.5	3.0	100	.06	Pn	1763.5	13.0	26.6	.041
-	-	-	-	-	Pn	807.5	3.0	151.5	1.0	-	-	-	-	-
Pe	30.5	0.65	400	1.2	Pe	389.0	3.0	5.5	.055	Pe	660.5	14.0	40	.046
-	-	-	-	-	Pe	389.0	3.0	131.5	.92	-	-	-	-	-
Lgz	29.9	2.675	10	.6	Lgz	1767.3	7.25	-	-	-	-	-	-	-
Lgn	33.8	2.575	15	1.0	Lgn	1311.4	7.25	-	-	-	-	-	-	-
Lge	53.2	2.675	10	.3	Lge	2362.1	6.5	-	-	-	-	-	-	-
-	-	-	-	-	Lrz	3815.6	9.0	6000	.05	Lrz	76476.5	31	6000	.035
-	-	-	-	-	Lrn	2316.9	10.75	333.	.04	Lrn	53901.2	28	450	.05
-	-	-	-	-	Lre	5671.6	11.75	1363.6	.03	Lre	105866	34	3750	.046

MRK MSNY Delta = 33.27, Azimuth = 216.85, 63/094/0017:38.6

	SP					MP					LP			
Phase	Amp	T(sec)	(S/N)	F(Hz)	Phase	Amp	T(sec)	(S/N)	F(Hz)	Phase	Amp	T(sec)	(S/N)	F(Hz)
Pz	137.9	0.925	60	1.15	Pz	332.9	1.5	40	.06	Pz	1642.6	17	100	.044
-	-	-	-	-	Pz	332.9	1.5	55	.99	-	-	-	-	-
Pn	67.9	0.925	30	1.3	Pn	185.1	1.25	31	.1	Pn	1210.3	20	300	.035
Pn	67.9	0.925	27.2	2.6	Pn	185.1	1.25	50	.955	-	-	-	-	-
Pe	39.6	1.0	25	2.5	Pe	1291.1	1.3	14.3	.05	Pe	630	17	150	.033
-	-	-	-	-	Pe	1291.1	1.3	40	.96	-	-	-	-	-
-	-	-	-	-	Lrz	4627	26	1111.1	.04	Lrz	151697	27	5555.5	0.39
-	-	-	-	-	Lrn	3472.3	24.25	1111.1	.04	Lrn	106931	24	20000	0.36
-	-	-	-	-	Lre	3312.7	31.5	3433.3	.035	Lre	136292	29	25000	0.35

MRK HSON Delta = 34.6, Azimuth = 102.96, 03/094/0617:38.6													
	SP					MP					LP		
Phase	Amp	T(sec)	(S/N)	F(Hz)	Phase	Amp	T(sec)	(S/N)	F(Hz)	Phase	Amp	T(sec)	(S/N)	F(Hz)
Pz	504.4	0.95	500	1.5	Pz	1325.3	2.0	75	.04	Pz	4106.6	22.0	200	.011
-	-	-	-	-	Pz	1325.3	2.0	333.3	.97	-	-	-	-	
Pn	156.1	1.025	300	1.9	Pn	625.1	2.3	100	.035	Pn	2596.6	23.0	125	.011
-	-	-	-	-	Pn	625.1	2.3	142.6	.97	-	-	-	-	
Pe	22.6	0.57	400	1.9	Pe	54.6	1.5	10	.04	Pe	252.9	17.0	150	.041
-	-	-	-	-	Pe	54.6	1.5	100	.66	-	-	-	-	
Lgz	72.7	3.25	54.5	.4	-	-	-	-	-	-	-	-	-	
Lgz	72.7	3.25	20	.6	-	-	-	-	-	-	-	-	-	
Lgn	23.4	2.80	26.6	.35	-	-	-	-	-	-	-	-	-	
Lge	57.3	3.025	40	.35	-	-	-	-	-	-	-	-	-	
Lge	57.3	3.025	30	1.2	-	-	-	-	-	-	-	-	-	
-	-	-	-	-	Lrz	4416.4	8.25	1400	.035	Lrz	55187.5	27.0	6000	.04
-	-	-	-	-	-	-	-	-	-	Lrz	55187.5	27.0	114.3	.051
-	-	-	-	-	Lrn	3110.3	8.5	2000	.035	Lrn	49576.6	31.0	4500	.056
-	-	-	-	-	-	-	-	-	-	Lrn	49576.6	31.0	100	1
-	-	-	-	-	Lre	4265.4	7.0	2000	.03	Lre	71655.5	40.0	14235.7	.025
-	-	-	-	-	-	-	-	-	-	Lre	71655.5	40.0	1570	.09

MRK HRND Delta = 38.86, Azimuth = 102.86, 03/094/0617:38.6													
	SP					MP					LP		
Phase	Amp	T(sec)	(S/N)	F(Hz)	Phase	Amp	T(sec)	(S/N)	F(Hz)	Phase	Amp	T(sec)	(S/N)	F(Hz)
Pz	108.7	1.525	30	1.3	Pz	649.7	3.25	350	.03	Pz	7921.3	25	909.6	.009
-	-	-	-	-	Pz	649.7	3.25	350	.03	Pz	7921.3	25	75	.03
Pn	129.7	1.575	666	1.3	Pn	553.1	2.85	700	.04	Pn	5990.4	25	333.3	.013
-	-	-	-	-	Pn	553.1	2.85	714	.65	Pn	5990.4	25	16.3	.03
Pe	74.7	1.2	66.6	1.1	Pe	130.6	1.75	100	.03	Pe	2073.4	25	200	.03
-	-	-	-	-	Pe	130.6	1.75	428.6	.66	Pe	2073.4	25	12.5	.09
Lgz	96.0	2.75	33.3	1.4	Lgz	1301.6	5.5	5000	.035	-	-	-	-	
Lgn	114.4	1.75	66.6	1.2	Lgn	1557.6	5.75	5000	.03	-	-	-	-	
Lge	179.3	2.975	50	1.1	Lge	6114.4	7.25	7000	.025	-	-	-	-	
-	-	-	-	-	Lrz	3449.6	12.75	6000	.05	Lrz	70761.3	32	10000	.035
-	-	-	-	-	-	-	-	-	-	Lrz	70761.3	32	333	.09
-	-	-	-	-	Lrn	4036.16	8.75	7500	.06	Lrn	35427.7	29	10000	.025
-	-	-	-	-	-	-	-	-	-	Lrn	35427.7	29	200	.095
-	-	-	-	-	Lre	6114.4	7.25	6000	.04	Lre	136789.026	55333	125	
-	-	-	-	-	-	-	-	-	-	Lre	136789.026	950	59	

NTS NBCP Delta = 84.51, Azimuth = 152.47, 82/217/1402:60.9

	SP					MP					LP			
Phase	Amp	T(sec)	(S/N)	F(Hz)	Phase	Amp	T(sec)	(S/N)	F(Hz)	Phase	Amp	T(sec)	(S/N)	F(Hz)
Pz	264	0.95	148.6	1.1	Pz	146	1.25	100	1.31	-	-	-	-	-
Pn	89	0.95	16.6	0.8	Pn	19	1.35	13.75	.75	-	-	-	-	-
-	-	-	-	-	Pn	19	1.25	16.0	1.3	-	-	-	-	-
Pe	66	0.85	80.0	10	Pe	66	1.1	37.5	.85	-	-	-	-	-
-	-	-	-	-	Pe	86	1.1	50.0	1.27	-	-	-	-	-
Lgz	88	2.45	22.5	.4	Lgz	167	2.5	11	.4	-	-	-	-	-
-	-	-	-	-	Lgz	167	2.5	10	.65	-	-	-	-	-
Lgn	880	2.65	80	.4	Lgn	706	2.75	50	.37	-	-	-	-	-
-	-	-	-	-	Lgn	706	2.75	62	.6	-	-	-	-	-
Lge	101	1.72	40	.4	Lge	162	3.0	30	.39	-	-	-	-	-
-	-	-	-	-	Lge	162	3.0	22.5	.6	-	-	-	-	-
-	-	-	-	-	Lrz	257	6.25	33	.15	-	-	-	-	-
-	-	-	-	-	Lrn	222	4.25	30	.36	-	-	-	-	-
-	-	-	-	-	Lre	194	5.0	50	.15	-	-	-	-	-

NTS NBNY Delta = 85.44, Azimuth = 152.54, 82/217/1402:60.9

	SP					MP					LP			
Phase	Amp	T(sec)	(S/N)	F(Hz)	Phase	Amp	T(sec)	(S/N)	F(Hz)	Phase	Amp	T(sec)	(S/N)	F(Hz)
Pz	102	1.085	100	0.8	Pz	253	2.0	110	1.3	Pz	26	20	2.9	.115
Pn	97	1.05	66.6	1.6	Pn	192	1.75	65.7	.77	Pn	-	-	6.4	0.75
Pe	14	0.6	67	1.7	Pe	11	1.25	50	.95	Pe	-	-	2.7	.062
Lgz	36	2.025	85	.4	Lgz	346	3.75	20	.23	-	-	-	-	-
Lgz	36	2.025	12.5	6.0	Lgz	346	3.75	20	.46	-	-	-	-	-
Lgn	81	2.6	16.1	.35	Lgn	176	3.5	16.1	.22	-	-	-	-	-
Lgn	81	2.6	11.1	7.6	-	-	-	-	-	-	-	-	-	-
Lge	66	2.075	80.	.4	Lge	261	3.25	33.3	.12	-	-	-	-	-
Lge	66	2.075	40.	6.0	Lge	261	3.25	35.0	.46	-	-	-	-	-
-	-	-	-	-	Lrz	264	6.0	41.6	.066	Lrz	1360	16	54	.05
-	-	-	-	-	Lrn	199	6.0	27.8	.13	Lrn	953	17	60	.065
-	-	-	-	-	Lre	250	6.5	36.3	.19	Lre	384	17	36	.115

NTS NBNY Delta = 31.95, Azimuth = 571.15, 82/217/1402:60.9

	SP					MP					LP			
Phase	Amp	T(sec)	(S/N)	F(Hz)	Phase	Amp	T(sec)	(S/N)	F(Hz)	Phase	Amp	T(sec)	(S/N)	F(Hz)
Pz	23	1.075	10	1.0	Pz	65	2.75	16	1.13	Pz	33	10	-	-
Pn	3.6	0.825	-	-	Pn	34	2.75	5	1.15	Pn	16	15	-	-
Pe	17	1.1	7	1.1	Pe	41	2.5	10	1.21	Pe	20	13	-	-
Lgz	37	1.975	15	.4	Lgz	146	2.75	10	.63	-	-	-	-	
Lgn	65	2.075	30	.4	Lgn	257	3.0	80	.96	Lg	-	-	-	
Lge	29	1.75	7.1	.5	Lge	106	2.5	8.6	.46	-	-	-	-	
Lge	-	-	-	-	Lge	106	2.5	13.3	.66	-	-	-	-	
Lrz	-	-	-	-	Lrz	765	10.85	62.5	.13	Lrz	2762	13	100	.09
Lrz	-	-	-	-	-	-	-	-	-	Lrz	2762	13	50	.113
Lrn	-	-	-	-	Lrn	135	7.0	16.8	.13	Lrn	485	13	24	.073
Lre	-	-	-	-	Lre	465	10.75	80	.14	Lre	2100	14	80	.06
Lre	-	-	-	-	-	-	-	-	-	Lre	2100	14	66.6	.151

| NTS MDCN Delta = 21.04, Azimuth = 237.71, 82/217/1402:02.0 | | | | | | | | | | | | | | |
| SP | | | | | MP | | | | | LP | | | | |
Phase	Amp	T(sec)	(S/N)	F(Hz)	Phase	Amp	T(sec)	(S/N)	F(Hz)	Phase	Amp	T(sec)	(S/N)	F(Hz)
Pz	734	0.975	666.6	1.3	Pz	629	1.5	600	1.3	Pz	44	11.0	6	.05
-	-	-	-	-	-	-	-	-	-	Pz	44	11.0	3.3	.162
Pn	245	0.95	466.6	1.3	Pn	604	1.5	350	1.3	Pn	22	9.0	5	.165
Pe	236	1.0	500	1.3	Pe	290	1.5	1666	1.21	Pe	16	11.0	5	.207
Lgz	495	2.05	30	.5	Lgz	226	2.75	33.3	.69	-	-	-	-	-
Lgz	496	2.05	33	10.5	-	-	-	-	-	-	-	-	-	-
Lgn	15	1.4	18.3	.66	Lgn	156	2.75	12.2	.66	-	-	-	-	-
Lgn	15	1.4	15.0	10.3	-	-	-	-	-	-	-	-	-	-
Lge	75	1.6	41.6	.7	Lge	284	2.25	44.4	.61	-	-	-	-	-
Lge	75	1.6	15.0	10.6	-	-	-	-	-	-	-	-	-	-
-	-	-	-	-	Lrz	477	7.25	75	.06	Lrz	671	13	50	.05
-	-	-	-	-	-	-	-	-	-	Lrz	671	13	54.5	.13
-	-	-	-	-	Lrn	340	6.75	60	.13	Lrn	622	13	57.1	.119
-	-	-	-	-	Lre	217	6.75	55.5	.18	Lre	413	13	35.7	.11

| NTS RSSD Delta = 11.48, Azimuth = 235.37, 82/217/1400:00.0 | | | | | | | | | | | | | | |
| SP | | | | | MP | | | | | LP | | | | |
Phase	Amp	T(sec)	(S/N)	F(Hz)	Phase	Amp	T(sec)	(S/N)	F(Hz)	Phase	Amp	T(sec)	(S/N)	F(Hz)
Pzz	293.1	0.675	450	1.1	Pz	229.1	1.75	466	.96	Pz	22.7	13.0	5.0	.255
Pzz	-	-	-	-	-	-	-	-	-	Pz	z	13.0	5.0	.335
Pzn	220.5	0.7	250	1.1	Pn	237.9	1.75	350	1.12	Pn	3.0	6.0	4.0	.255
Pzn	-	-	-	-	-	-	-	-	-	Pn	3.0	6.0	10.0	.34
Pze	255.6	0.925	525	1.1	Pe	284.6	1.75	350	.9	Pe	12.3	11.0	8.3	.255
Pze	-	-	-	-	-	-	-	-	-	Pe	12.3	11.0	6.6	.34
Lgz	339	1.5	600	.7	Lgz	673	2.25	6671	.64	-	-	-	-	-
Lgn	352	1.425	265	.7	Lgn	686	2.25	200	.55	-	-	-	-	-
Lge	265	1.45	250	1.3	Lge	656	1.75	200	.66	-	-	-	-	-
-	-	-	-	-	Lrz	815	6.5	100	.14	Lrz	3565	15	16	.015
-	-	-	-	-	Lrn	696	4.5	60	.17	Lrn	1555	15	8.8	.085
-	-	-	-	-	Lrn	696	4.5	100	.66	-	-	-	-	-
-	-	-	-	-	Lre	716	6.75	125	.1	Lre	2407	14	12.5	.085
-	-	-	-	-	Lre	716	6.75	166.6	.5	-	-	-	-	-

NY ????? Delta = 16.03, Azimuth = 136.51, 63/087/1983:33.4														
SP					**MP**					**LP**				
Phase	Amp	T(sec)	(S/N)	F(Hz)	Phase	Amp	T(sec)	(S/N)	F(Hz)	Phase	Amp	T(sec)	(S/N)	F(Hz)
Pz	-	-	-	-	Pz	-	-	-	-	Pz	-	-	-	-
Pn	-	-	-	-	Pn	Cal	-	-	-	Pn	Cal	-	-	-
Pe	-	-	-	-	Pe	-	-	-	-	Pe	-	-	-	-
Lgz	4.8	2.185	-	-	Lgz	-	-	-	-	-	-	-	-	-
Lgn	7.1	1.875	60	2.0	Lgn	-	-	-	-	-	-	-	-	-
Lge	4.95	2.2	-	-	Lge	-	-	-	-	-	-	-	-	-

NY ????? Delta = 3.63, Azimuth = 197.03, 63/087/1983:33.4														
SP					**MP**					**LP**				
Phase	Amp	T(sec)	(S/N)	F(Hz)	Phase	Amp	T(sec)	(S/N)	F(Hz)	Phase	Amp	T(sec)	(S/N)	F(Hz)
Pz	10.4	0.2	10.5	5.7	Pz	-	-	5.4	.92	Pz	-	-	-	-
Pz	10.4	0.2	11.6	7.4	-	-	-	-	-	-	-	-	-	-
Pn	7.3	0.175	10	4.8	Pn	Cal	-	-	-	Pn	Cal	-	-	-
Pn	7.3	0.175	15.6	6.5	-	-	-	-	-	-	-	-	-	-
Pe	3.1	0.15	8.1	4.7	Pe	-	-	-	-	Pe	-	-	-	-
Lgz	64.6	0.2	50	4.8	Lgz	-	-	5.0	1.4	-	-	-	-	-
Lgn	54.5	0.2	100	5.0	Lgn	-	-	-	-	-	-	-	-	-
Lge	76.9	0.225	100	5.0	Lge	-	-	13.3	1.04	-	-	-	-	-

APPENDIX II

DYNAMIC-KINEMATIC CRITERIA FOR EVENT REALITY

A BETTER APPROACH TO HANDLING AMPLITUDE DATA AA

M E M O R A N D U M

TO: A. Kerr, W. Dean, J. Goncz, R. North, R. Slunga, R. Shumway

FROM: R. Blandford

SUBJECT: Dynamic-Kinematic Criteria for Event Reality

DATE: 7 October 1982

We now have a complete "system" for dynamic-kinematic amplitude checking; attached to this memo. I think this system could be checked out fairly well with the artificial data John Goncz and I are generating. The subroutine amp may diverge if very large or small TD = 1 type values are in the data. Bob Shumway and I will soon distribute an improved version of amp. I think this code is in a "final" state suitable for use in existing AA programs. Only the I/O needs to be modified, and this is fairly well isolated in the event.f and mkpkin.f files.

As long as we are talking about AA, I propose a measure of AA quality, "Association Percentage" defined as follows. Define events which are to be detected; e.g. events with 5 non-array stations; plus events with two arrays and one confirming station, plus events with 2 P waves and one S, etc. All arrivals in this set of events when perfectly analyzed constitute the "base set of arrivals". Now we go down the perfect bulletin and pick out the first event. Is there an event in the AA with (75%) of the arrivals. (Obviously 75% is a variable; probably anywhere between 60% and 90% is alright.) If so, then all correct arrivals in that AA event may be added to the total correct arrivals count; and all incorrectly associated arrivals should be subtracted. I propose that a correctly associated arrival should count even if the phase name is incorrect. (Or perhaps it should get 1/2 or 0 weight if incorrectly identified.) In this way all "perfect bulletin" events are considered. Any remaining arrivals which have been associated into events (which are, presumably "false" or "bad" events and which will give an analyst severe trouble to clean up) will be subtracted from the total correct arrivals count. The Association Percentage is calculated as (total correct arrivals count)/(base set of arrivals).

This measure:

Doubly penalizes the creation of false events and incorrect
  association to good events.
Rewards correct identification of later phases.
Does not depend on location error which is highly variable depending
  on event size and travel-time residuals.
Can be easily calculated automatically.
Perhaps too severely penalizes splitting large events, especially an
  equal split.

INTRODUCTION

The problem of verifying that magnitude estimators for events which have been created by an automatic association (AA) routine are based on a reasonable subset of detecting and non-detecting stations has been considered by Elvers (1980). She developed a "plausibility function" for the amplitude distributions which is essentially proportional to the likelihood of observing a particular configuration of amplitudes when the event is assumed to have occurred.

In this discussion, we attempt to improve several aspects of this procedure. As a computational improvement we also have developed a Newton-Raphson procedure for computing the maximum likelihood magnitude, assuming the signal and noise variances are known. This procedure runs much faster than the search techniques used by previous authors.

We also give a method for discarding single stations with outlying amplitudes (I, see Figure 1) based on the "influence" they exert on the magnitude estimator. This replaces the Elvers procedure of comparing the separate components of the likelihood for the purpose of determining the influential stations. Our procedure for discarding stations is also apparently not so likely to "destroy" the event in the case that a large number of stations are "down" and fail to report, but do not inform the bulletin analysis center of this fact.

Slunga (personal communication, 1982) has pointed out that the "dynamic" amplitude criteria of Elvers seem to erroneously discard arrivals from an event on the basis of amplitude anomalies. On occasion, although the amplitudes are indeed anomalous, the probability that the arrival time could agree by accident seems even smaller, so that it seems unreasonable to totally discard the arrival from the event.

To help remedy this paradox we propose to measure the overall event plausibility with a "kinematic" likelihood ratio (II) in parallel with the dynamic one. If the dynamic criteria suggest that an observed amplitude is unreliable but the kinematic criteria are favorable, then we suggest that the appropriate procedure in most cases is to assume

that there is some error in the amplitude measurement and to recalculate
the magnitude, after making an appropriate change in the amplitude data,
but to continue to use the reported arrival time for estimation of
location.

Finally, we have developed a procedure for tying these new
computational techniques together. In general terms this procedure is
not derived from theoretical considerations but embodies common sense
ideas about the causes of erroneous amplitude measurements.

It is important to emphasize that these techniques cannot simply be
inserted into an automatic association program as mathematical routines
like, for example, the cosine function. Instead the routines contain
parameters which are specific to the network, detectors, and methods of
analysis. These parameters must be determined by careful statistical
analysis of network bulletins which are relatively error-free, and by
analysis of false events produced by the automatic association program
in which they are to be used.

FUNCTIONAL DESCRIPTION

In Figure 1 we see a flow chart of the proposed procedure. The Roman numerals I-II denote the computational techniques referred to in the Introduction.

At the top of Figure 1 we see that the event is submitted to the program for analysis. Obviously only those events should be accepted for which the program is prepared. For example we may anticipate that the first version of the program will be prepared to work only on initial P waves. If the event is made up of Pg, S, Lg, etc. then the algorithm has nothing to contribute. On the other hand an event with only one P wave and without an amplitude reading may be submitted. The single detection might be unlikely because many stations with lower thresholds nearby the detecting station did not detect. When this P wave is discarded then the event might be unreliable on kinematic grounds.

The event data is then submitted to a subroutine (I) which computes the Ringdal magnitude and detects outlying magnitudes. In Appendix I is a discussion and listing of a subroutine (amp) which rapidly computes the Ringdal magnitude given station amplitudes and thresholds in terms of magnitudes, and assuming that the signal and noise variances are known. Before this subroutine can be used, of course, distance-amplitude relations must be used to transform amplitudes and thresholds to magnitudes.

The amplitude patterns can be subdivided roughly into n_1 observed amplitudes, n_2 above the noise threshold and with arrival times but not amplitudes reported, and n_3 below the noise threshold and not detected. Of course other subcategories such as clipping might be added. For the general unknown magnitude case the log-likelihood as given by Elvers (1980) would be of the form:

$$\ln L(m) \doteq -\frac{n_1}{2}\ln\sigma_s^2 - \frac{1}{2\sigma_s^2}\sum_{j=1}^{n_1}(m_j - m)^2 + \sum_{j=1}^{n_2}\ln\Phi(t_j) + \sum_{j=1}^{n_3}\ln\Phi(-\varepsilon_j)$$

(1)

FLOW CHART FOR DYNAMIC-KINEMATIC ANALYSIS FOR AUTOMATIC ASSOCIATION

Enter Event

"Large" effect on $\hat{m}_b$ for some station?

I

N → G

Y

$(P_k^{-1} \text{ real}) < 0.95$

II

B — N →

Determine Event Type

Detecting Station?

N

Y

Discard Station

N — Amplitude Measured?

Y

Change Station type to " > noise"
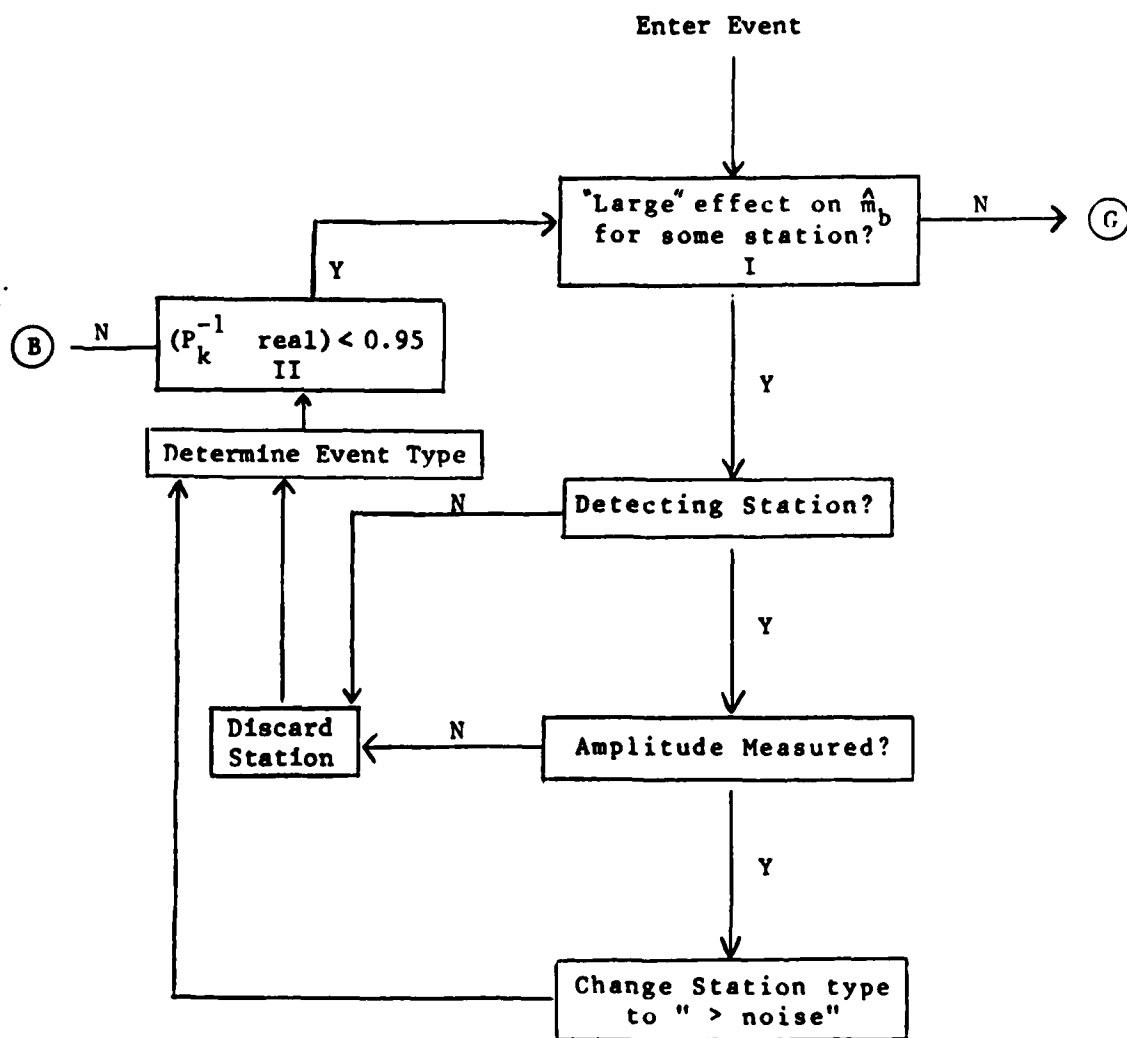
Pa - Amplitude probability	G - Good event exit
Pk^{-1} - Kinematic probability with one less station if a suspect station has been removed	B - Bad event exit

Figure 1.
-64-

where m_j are the observed amplitudes, m is the theoretical magnitude
and:

$$z_j = \frac{m - \bar{D}_j - C}{\sqrt{\sigma_s^2 + \sigma_j^2}}$$

is a standard value depending on the mean noise level $\bar{D}_j$ with variance
σ_j^2, the theoretical magnitude m with observed variance σ_s^2, and a
signal-to-noise constant C. Since m is the only unknown, (1) can be
maximized using the Newton-Raphson or scoring algorithms, which leads to
the maximum likelihood estimator m and its estimated variance $\hat{\sigma}_m^2$ (see
Appendix I). .The above approach is essentially that followed by Elvers
(1980).

As a modification to the above Elvers (1980) suggests comparing the
value of the maximized log likelihood, say ln $L(\hat{m})$ with some arbitrary
threshold, with the first component of (1) modified to behave like an
estimated interval probability. If the total plausibility, say ln $L(\hat{m})$
is too small, then the event can be rejected. The other decision that
can be made at this point in the Elvers procedure is to discard a single
station value based on a single station component of ln $L(\hat{m})$. For
example the decision to reject a station j which does not observe is
based on the value of $\ln(\Phi(-z_j))$, which is the probability of observing
a value below the noise threshold at the jth station.

The problem, mentioned by Elvers (1980), with this approach is that
the total plausibility depends in part upon point values of the density
and in part upon interval probabilities which are integrated densities.
Thus it is likely that eliminating an event purely on this criterion
will unnecessarily eliminate events. The problem is magnified when one
uses the Elvers (1980) procedure to eliminate single stations; purely on
the basis of their plausibility values.

As a better method for detecting station outliers, we suggest
recalculating the magnitude estimator with each station value missing to
obtain, say $m_{(-i)}$ for i=1,...,n, where $m_{(-i)}$ denotes the magnitude
estimated when station i is left out of the calculation. These can be
compared with the original estimator, say m, to determine the "influence

of station i. For example, a common measure of influence is "Cook's distance", defined in this case by:

$$z_{(-i)} = \frac{\hat{m} - \hat{m}_{(-i)}}{\hat{\sigma}_{\hat{m}}} \qquad (2)$$

An heuristic procedure suggested by Cook is to reject station i when $z_{(-i)}$ moves further away from zero than $z(\alpha/2)$, where α is some arbitrary probability value.

As an example of how the two procedures for amplitude verification might work in practice, consider the 11 station "event", shown schematically in Table 1. We note first that taking the simple mean of the observed magnitudes yields $\bar{m} = 4.04$, whereas the maximum likelihood estimator is $\hat{m} = 3.78$ with estimated standard deviation $\hat{\sigma}_{\hat{m}} = .12$ so that the censored observations definitely pull the estimator down.

In order to determine whether any of the station values m_i are outliers, we may use the analogue of Cook's distance given in equation (2). The estimated deleted station magnitudes $\hat{m}_{(-i)}$ for i=1,2,...,11 are shown in Table 1 and we note that the greatest change is produced by omitting station 6($\hat{m}_{-6} = 3.89$) which is the value known to be below its noise threshold $\bar{b}_3 = 3$. The elimination of this station then moves the maximum likelihood estimator back towards the mean.

A program, DETZ, which produces the values of $z_{(-i)}$ is given in Appendix I.

TREATMENT OF STATIONS WITH ANOMALOUS AMPLITUDES

Returning to Figure 1 we must ask what course of action to take when an anomalous station amplitude is discovered by procedure I. First we determine if the most anomalous station has reported a detection or if, as in Table 1, it has simply failed to report at all, implying that the signal level is below the noise level. In the latter case we follow the approach suggested by Elvers (1980) and simply discard the station. However, we may look ahead a bit and note that, unlike Elvers we

-66-

TABLE 1

MAXIMUM LIKELIHOOD ESTIMATORS FOR MAGNITUDE

Case I	i	Data	$\hat{m}_{-i}$	$\hat{\sigma}_{\hat{m}}$	lnL	$z_{(-i)}$
Station	1	4.0	3.74	.13	1.03	.32
	2	3.6	3.80	.12	.96	-.25
	3	4.4	3.67	.13	2.27	.89
	4	4.0	3.74	.13	1.03	.32
	5	4.2	3.70	.13	1.51	.60
*	6	3.0	3.89	.17	6.14	-1.00
	7	4.0	3.80	.12	3.06	-.23
	8	4.2	3.79	.12	2.87	-.14
	9	3.9	3.81	.12	3.20	-.29
	10	4.5	3.78	.12	2.73	-.05
	11	5.0	3.78	.12	2.68	-.00
	Overall		3.78	.12	2.68	

immediately test for the kinematic probability of this event (II) and if the probability of the event being real is less than say 0.95 then we exit the routine with a bad event flag. That is, non-detection by this station suggests that there is something wrong with the event, and unless the kinematic probability is high the event is discarded. On the other hand, if the kinematic probability of the event is high, then probably there was something wrong at the station, and we return to further analyze the event without considering this station. Since in practice many stations fail to report due to operational consideration we should probably set a less restictive threshold for the non-detecting stations, that is, we should tend to reject them first. For example, if for a non-detecting station $z_{(-i)} \leq -0.7$ reject it (see Table I) but otherwise require $z_{(-i)} \geq 1.0$ for rejection. Probably we should have no anomalous non-detecting station remaining before considering other stations. Further work, perhaps empirical is needed to best determine those thresholds.

If the anomalous station did detect we ask if an amplitude was measured or not. If no amplitude was measured then we must have the situation where this station could not have been expected to detect; typically a station in a shadow zone to a small event. Again we discard the station and check the kinematic probability. Since we have by this time eliminated many of the incorrectly non-reporting stations, the event magnitude should not be biased too low so that stations should not be incorrectly thrown out at this point.

Finally we have the case where there is an amplitude measurement at the anomalous station: either it is too large or too small. In either case we assume that some blunder has been made and that if a true signal has been detected then the amplitude has been recorded or transmitted incorrectly. Thus we simply change the amplitude measurement (not in the original files of course) to state that the signal was greater than the noise. Again we proceed through the kinematic criterion. Note that if this event comes around again then this detection will not have a measured amplitude so that if it is unlikely that this station could have detected the event at all the arrival will be discarded.

KINEMATIC REJECTION CRITERIA (II)

The kinematic criteria for the event existence are to be established
as follows. First, it is necessary to establish event types which will
consist of the number of array stations and the number of non-array
stations detecting. These stations may also have to be broken down by
the criteria of analyst and automatic detection. For each type of event
we may determine the ratio of good events to false events of each type
in each day. This ratio then gives directly the probability that an
event of each type is real.

PROCESSING AFTER DYNAMIC CHECKING

If any detections have been discarded then the reduced set of
arrivals should be used to generate a new trial epicenter. If the same
final set of arrivals should result then the iteration should be
suspended. Care needs to be taken to avoid an infinite loop.

REFERENCES

Elvers, E. (1980). International Seismological Data Center: Procedures
to check events through dynamic information and to estimate
magnitudes, FOA Report C 20368-Tl. Forsvarets Forskningsanstalt
Huvudavdelning 2, Stockholm, Sweden.

Ringdal, F. (1976). Maximum likelihood estimation of seismic magnitude,
Bull. Seism. Soc. Am., 66, 789-802.

Slunga, R. (1980). An algorithm for associating reported arrivals to a
global seismic network into groups defining seismic events, FOA
Report C 20386-Tl, Forskningsanstalt Huvudavdelning 2, Stockholm,
Sweden.

APPENDIX I

We have developed a Newton-Raphson algorithm for maximizing $\ln L(m)$ by noting that:

$$\frac{d \ln L(m)}{dm} = \frac{n_1}{\sigma_s^2}(\bar{m}-m) + \sum_{j=1}^{n_2} \frac{R(z_j)}{\omega_j} - \sum_{j=1}^{n_3} \frac{R(-z_j)}{\omega_j}$$

(A1)

where

$$R(z_j) = \frac{\varphi(z_j)}{\Phi(z_j)}$$

(A2)

and

$$\omega_j = \sqrt{\sigma_s^2 + \sigma_j^2}$$

(A3)

where z_j given by the equation in the main text with:

$$\Phi(z) = \int_{-\infty}^{z} \varphi(x)\, dx$$

(A4)

and

(A5)

$$\varphi(x) = (2\pi)^{-\frac{1}{2}} \exp\left(-\frac{x^2}{2}\right)$$

Also:

$$\frac{\partial^2 \ln L(m)}{dm} = -\frac{n_1}{\sigma_s^2} - \sum_{j=1}^{n_2} \frac{(z_j R(z_j') + R^2(z_j'))}{w_j^2} - \sum_{j=1}^{n_3} \frac{(z_j R(z_j') + R^2(-z_j'))}{w_j^2}$$

Then the Newton-Raphson interations are of the form

$$m_{i+1} = m_i - \frac{\left(\frac{\partial \ln L(m)}{dm}\right)_{m_i}}{\left(\frac{\partial^2 \ln L(m)}{dm^2}\right)_{m_i}} \tag{A6}$$

with the final estimator $\hat{m}$ having an estimated standard error given by

$$\hat{\sigma}_{\hat{m}} = \left(-\frac{1}{\left(\frac{\partial^2 \ln L(m)}{dm^2}\right)_{\hat{m}}}\right)^{1/2} \tag{A7}$$

MEMORANDUM

TO: J. Goncz

FROM: R. Blandford ʔ ι

SUBJECT: A Better Approach to Handling Amplitude Data in AA

DATE: 19 April 1983

1. Compute maximum likelihood m_b using the observing stations plus a
    fixed set of about 20 reliable stations. An m_b is calculated with
    each station omitted in turn. Assume an <u>a-priori</u> $\sigma = 0.35\ m_b$
    throughout.

2. Analyze each of the above stations in screen as we do now, get the
    total number of points, then:

    i. If the station <u>did not</u> detect but

$$p(det) > .95, -1 \text{ point}$$
$$p(det) > .99, -2 \text{ points}$$

        Comments: If $p(det) > .95$ at many stations most stations will
        have detected if the event is big and loss of points for the
        occasional random non-detection will not matter. If the event
        is weak, only a <u>few</u> close stations will have $p(det) > 0.95$ so
        the occasional random non-detection is again unlikely to lose
        points.

    ii. If the station <u>did</u> detect and if, based on noise and m_b alone

$$p(det) < .01, -(\text{all points due to station})$$

        Comments: If the event is big there will be so many points that
        occasionally losing one will not be serious. If it is a small
        event and just trapped (correctly) the one distant station, then
        the probability of that happening for any particular one out of
        the 20 distant stations may be smaller than .05 so for that
        reason we set this threshold at .01 so that only about 1/5 of
        these events·will be incorrectly rejected. It is important to
        reject <u>all</u> the points due to the station, i.e. those due to
        azimuth and slowness and those due to local flags and associated
        S phases.

    iii. If the station <u>did</u> detect, and reports an amplitude A_o, and if,
          based on noise and m_b alone,

$$p(det) > .01 \quad \text{and}$$
$$p(amp > A_o) < .01 \quad \text{or}$$
$$p(amp < A_o) < .01 \quad \text{then}$$

discard amplitude, A_o (are left with estimated noise) and return to (1)

Comments: That is, compute all the negative points and m_b values over because the bad amplitude probably distorted all the m_b values. Note that this procedure does not "fiddle" with an event. It either results in complete acceptance or discards the event so that the kinematic processing has a new chance to do better.

RRB/paw

RECIPIENT   NUMBER OF COPIES

DEPARTMENT OF DEFENSE

DARPA/GSD   2
1400 Wilson Boulevard
Arlington, VA 22209

DARPA/PM   1
1400 Wilson Boulevard
Arlington, VA 22209

Defense Technical Information Center   12
Cameron Station   2
Alexandria, VA 22314

Defense Intelligence Agency   1
Directorate for Scientific and
  Technical Intelligence
Washington, D.C. 20301

Defense Nuclear Agency   1
Shock Physics Directorate/SS
Washington, D.C. 20305

Defense Nuclear Agency/SPSS   1
ATTN: Dr. Michael Shore
6801 Telegraph Road
Alexandria, VA 22310

DEPARTMENT OF THE AIR FORCE

AFGL/LW   1
ATTN: Dr. J. Cipar
Terrestrial Sciences Division
Hanscom AFB, MA 01730

AFOSR/NPG   1
ATTN: Director
Bldg 410, Room C222
Bolling AFB, Washington D.C. 20332

AFTAC/TG   3
Patrick AFB, FL 32925

AFTAC/TD (STINFO)   1
Patrick AFB, FL 32925

AFWL/NTESC   1
Kirtland AFB, NM 87171

DEPARTMENT OF THE ARMY

US Army Engineers   1
ATTN: Mr. J. Drake
Waterways Experiment Station
P.O. Box 631
Vicksburg, MS 39181

DEPARTMENT OF THE NAVY

NORDA   1
ATTN: Dr. J. A. Ballard
Code 543
NSTL Station, MS 39529

DEPARTMENT OF ENERGY

Department of Energy   1
ATTN: Dr. F. Dickerson (DP-52)
International Security Affairs
1000 Independence Avenue
Washington, D.C. 20545

Lawrence Livermore National Laboratory   2
ATTN: Dr. J. Hannon and Dr. M. Nordyke
University of California
P.O. Box 808
Livermore, CA 94550

Los Alamos Scientific Laboratory   1
ATTN: Dr. K. Olsen
P.O. Box 1663
Los Alamos, NM 87544

Sandia Laboratories   1
ATTN: Mr. P. Stokes
Geosciencies Department 1255
Albuquerque, NM 87115

OTHER GOVERNMENT AGENCIES

Central Intelligence Agency   1
ATTN: Dr. L. Turnbill
OSI/NED, Room 5G48
Washington, D.C. 20505

2

U.S. Arms Control and Disarmament Agency   2
ATTN: Mrs. M. Hoinkes
Division of Multilateral Affairs
Washington, D.C. 20301

U.S. Geological Survey   1
ATTN: Dr. T. Hanks
National Earthquake Research Center
345 Middlefield Road
Menlo Park, CA 94025

U.S. Geological Survey   1
ATTN: Dr. Robert Masse
Global Seismology Branch
Box 25046, Stop 967
Denver Federal Center
Denver, CO 80225

UNIVERSITIES

University of California, Berkeley   1
ATTN: DR. T. McEvilly
Department of Geology and Geophysics
Berkeley, CA 94720

California Institute of Technology   1
ATTN: Dr. D. Harkrider
Seismological Laboratory
Pasadena, CA 91125

University of California, San Diego   1
ATTN: Dr. J. Orcutt
Scripps Institute of Oceanography
La Jolla, CA 92093

Columbia University   1
ATTN: Dr. L. Sykes
Lamont-Doherty Geological Observatory
Palisades, NY 10964

Massachusetts Institute of Technology   3
ATTN: Dr. S. Soloman, Dr. N. Toksoz, Dr. T. Jordan
Department of Earth and Planetary Sciences
Cambridge, MA 02139

University of Nevada, Reno   1
ATTN: Dr. A. Ryall
Seismological Laboratory
Reno, NV 89557

The Pennsylvania State University   1
ATTN: Dr. S. Alexander
Department of Mineral Sciences
University Park, PN 16802

3

Southern Methodist University   1
ATTN: Dr. E. Herrin
Geophysical Laboratory
Dallas, TX 75275

CIRES   1
ATTN: Dr. C. Archambeau
University of Colorado
Boulder, CO 80309

Georgia Institute of Technology   1
ATTN: Professor Anton Dainty
The School of Geophysical Sciences
Atlanta, GA 30332

St. Louis University   1
ATTN: Dr. O. Nuttli
Department of Earth and Atmospheric Sciences
3507 Laclede
St. Louis, MO 63156

DEPARTMENT OF DEFENSE CONTRACTORS

Applied Research Associates, Incorporated   1
ATTN: Dr. N. Higgins
2101 San Pedro Boulevard North East
Suite A
Albuquerque, NM 87110

Applied Theory, Incorporated   1
ATTN: Dr. J. Trulio
930 South La Brea Avenue
Suite 2
Los Angeles, CA 90036

Center for Seismic Studies   2
ATTN: Dr. Carl Romney, and Dr. William Dean
1300 N. 17th Street, Suite 1450
Arlington, VA 22209

ENSCO, Incorporated   1
ATTN: Mr. G. Young
5408A Port Royal Road
Springfield, VA 22151

ENSCO, Incorporated   1
ATTN: Dr. R. Kemerait
1930 Highway A1A
Indian Harbour Beach, FL 32937

4

Pacific Sierra Research Corporation   1
ATTN: Mr. F. Thomas
12340 Santa Monica Boulevard
Los Angeles, CA   90025

Physics Applications, Incorporated   1
ATTN: Mr. C. Vincent
2340 Harris Way
San Jose, CA   95131

R&D Associates   1
ATTN: Dr. E. Martinelli
P.O. Box 9695
Marina del Rey, CA   90291

Rockwell International   1
ATTN: Dr. B. Tittmann
109 Camino.Dos Rios
Thousand Oaks, CA   91360

Gould Incorporated   1
ATTN: Mr. R. J. Woodard
Chesapeake Instrument Division
6711 Baymeado Drive
Glen Burnie, MD   21061

Rondout Associates, Incorporated   1
ATTN: Dr. P. Pomeroy
P.O. Box 224
Stone Ridge, NY   12484

Science Applications, Incorporated   1
ATTN: Dr. H. Pratt
P.O. Box 2351
La Jolla, CA   92038

Science Horizons
ATTN: Dr. T. Cherry and Dr. J. Minster   2
710 Encinitas Blvd
Suite 101
Encinitas, CA   92024

Sierra Geophysics, Incorporated   2
ATTN: Dr. R. Hart and Dr. G. Mellman
15446 Bell-Red Road
Redmond, WA   98052

SRI International   1
333 Ravensworth Avenue.
Menlo Park, CA   94025

5

S-Cubed
ATTN: Dr. Steven Day Dr. J. Savino   2
P.O. Box 1620
La Jolla, CA   92037

S-Cubed   1
ATTN: Mr. J. Murphy
11800 Sunrise Valley Drive
Suite 1112
Reston, VA   22091

Teledyne Geotech
ATTN: Dr. Z. Der and Mr. W. Rivers   2
314 Montgomery Street
Alexandria, VA   22314

Woodard-Clyde Associates   1
ATTN: Dr..Larry Burdick
380 West Del Mar Boulevard
Pasadena, CA   91105

Weidlinger Associates   1
ATTN: Dr. J. Isenberg
3000 Sand Hill Road
Building 4, Suite 245
Menlo Park, CA   94025

                        NON-U.S. RECIPIENTS

National Defense Research Institute   1
ATTN: Dr. Ola Dahlman
Stockholm 80, Sweden

Blacknest Seismological Center   1
ATTN: Mr. Peter Marshall
Atomic Weapons Research Establishment
UK Ministry of Defense
Brimpton, Reading RG7-4RS
United Kingdom

NTNF NORSAR   1
ATTN: Dr. Frode Ringdal
P.O. Box 51
N-2007 Kjeller
Norway

6

END

FILMED

11-84

DTIC